ATLAS Measurements of Photo-nuclear Processes in Ultra-Peripheral Pb+Pb Collisions

Ben Gilbert
On behalf of the ATLAS Collaboration

Introduction: Photo-nuclear Processes

In ultra-relativistic heavy ion collisions, the intense electromagnetic fields of the colliding ions provide a flux of quasi-real photons.

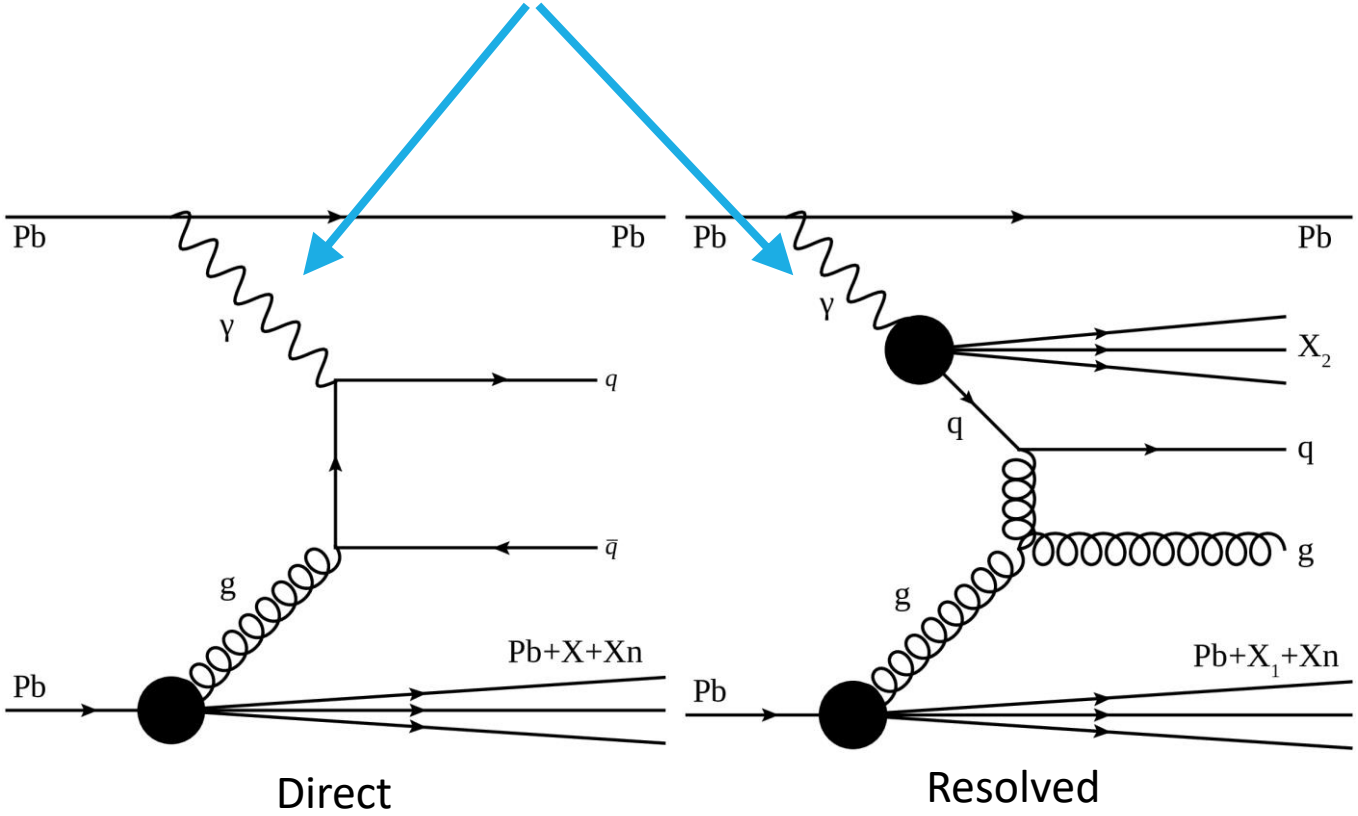

Direct

Resolved

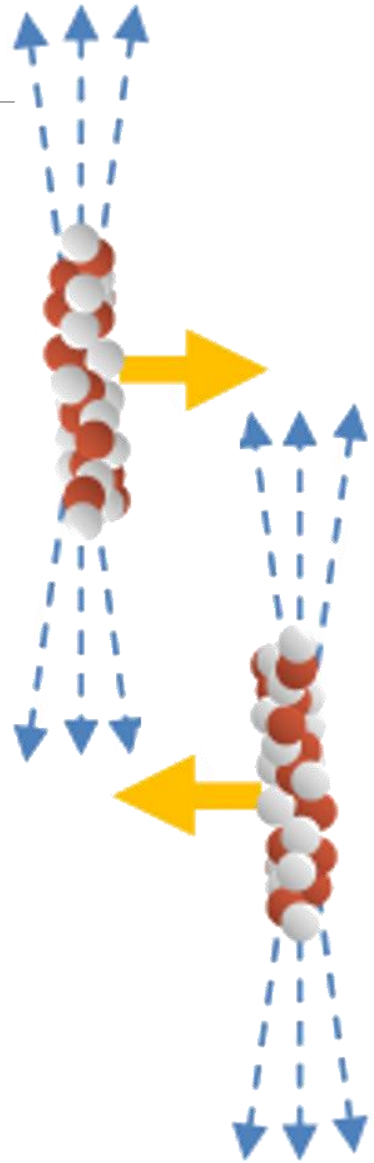

Introduction: Photo-nuclear Processes

In ultra-relativistic heavy ion collisions, the intense electromagnetic fields of the colliding ions provide a flux of quasi-real photons.

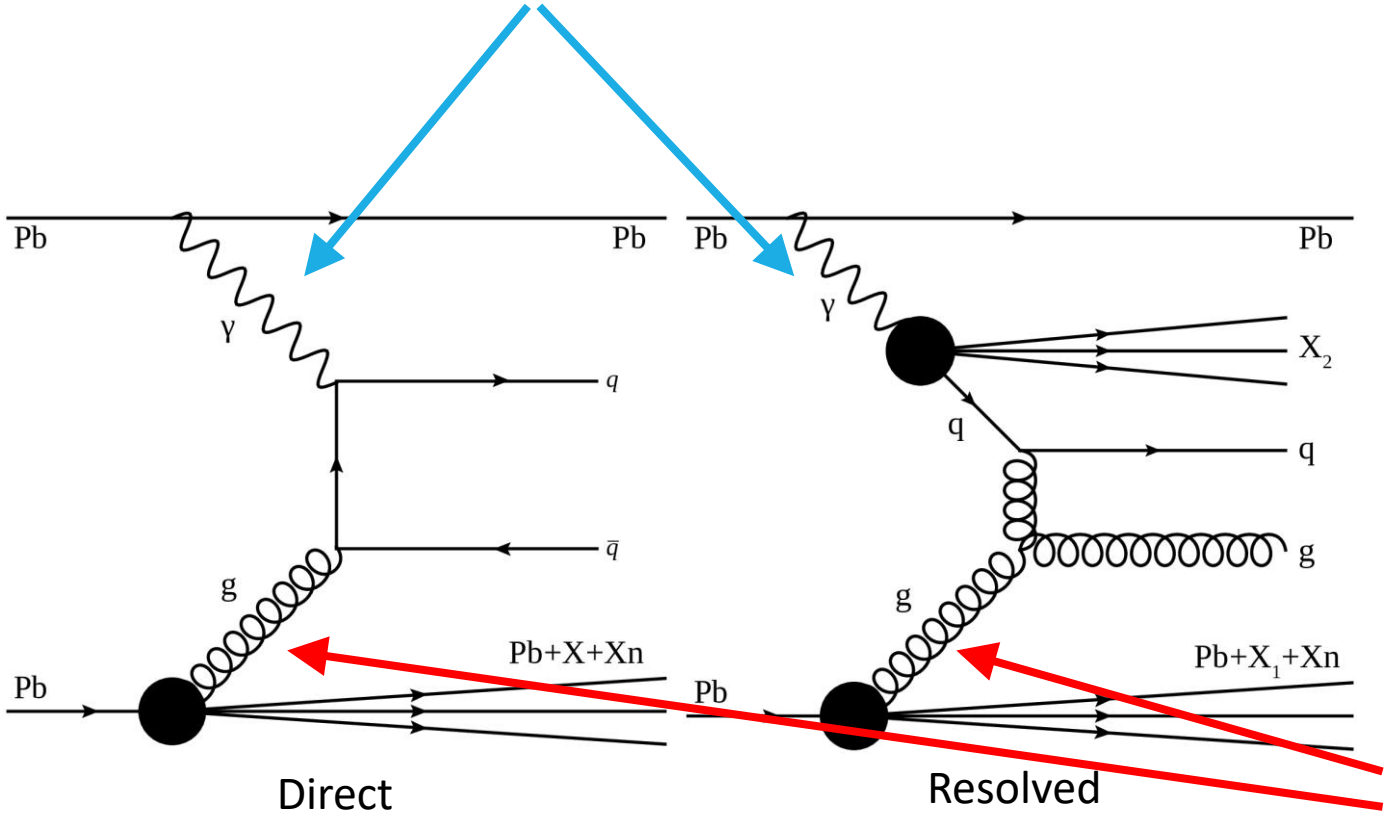

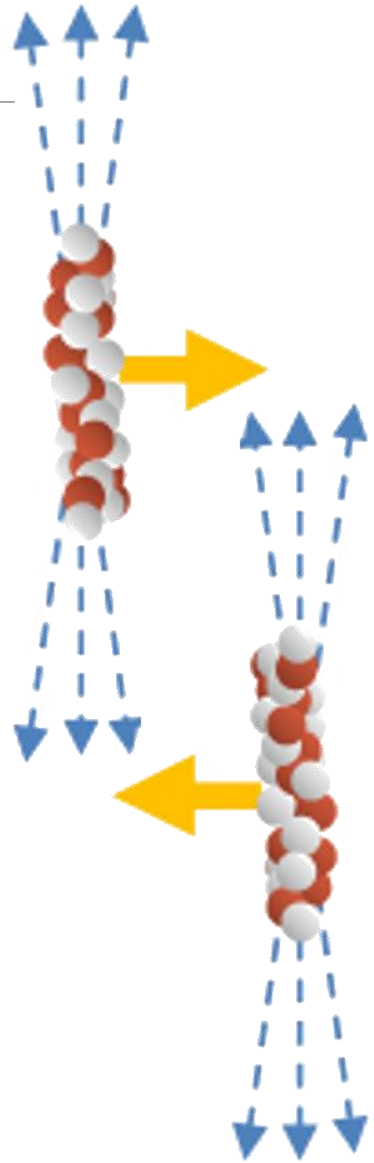

Those photons can scatter off of partons in the other (target) nucleus

Introduction: Photo-nuclear Processes

In ultra-relativistic heavy ion collisions, the intense electromagnetic fields of the colliding ions provide a flux of quasi-real photons.

"Direct" photons scatter off the nucleus.

"Resolved" photons scatter hadronically through a virtual excitation of the photon.

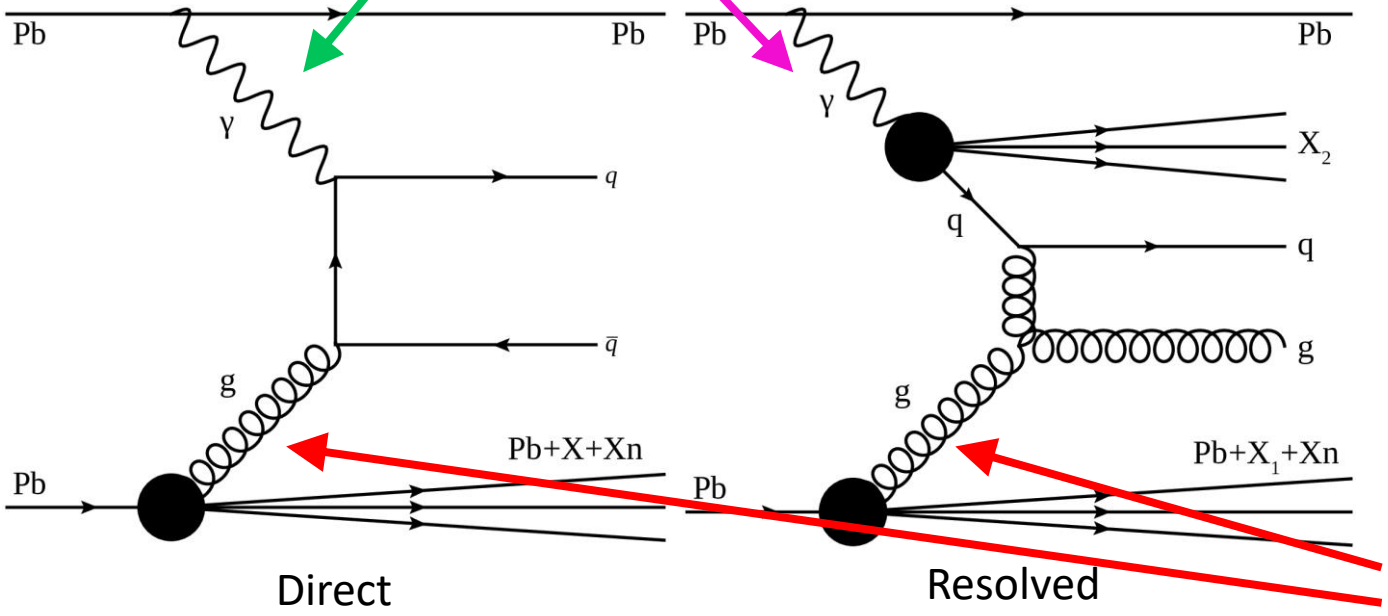

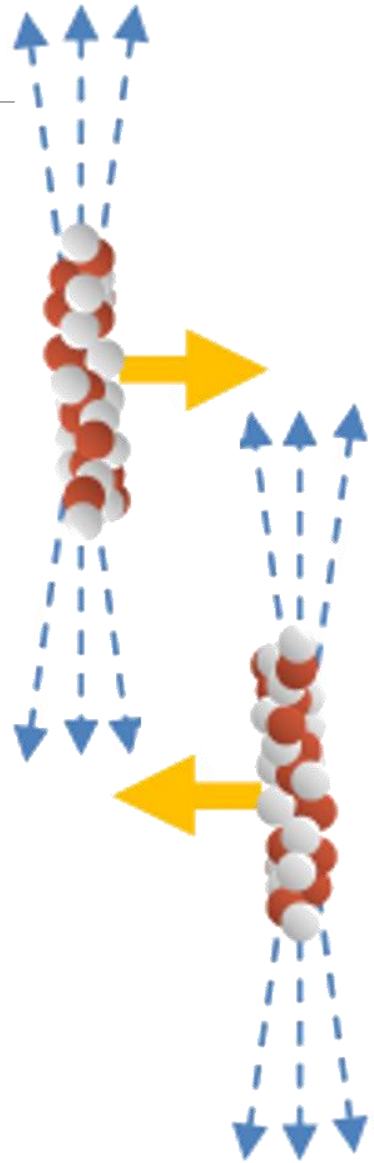

Those photons can scatter off of partons in the other (target) nucleus

Introduction: Photo-nuclear Processes

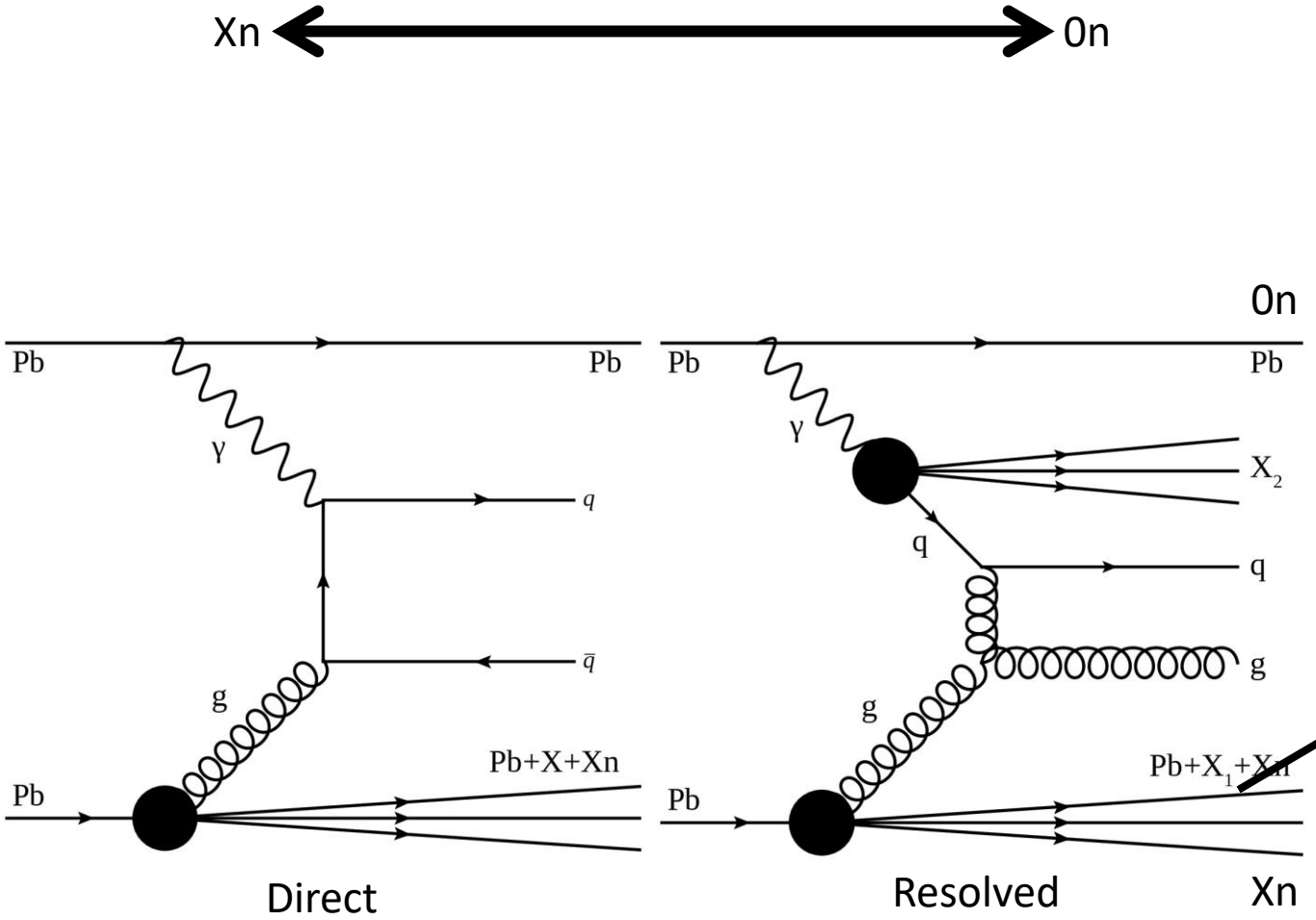

0nXn requirement for nuclear breakup in exactly one ATLAS Zero-Degree Calorimeter (ZDC)

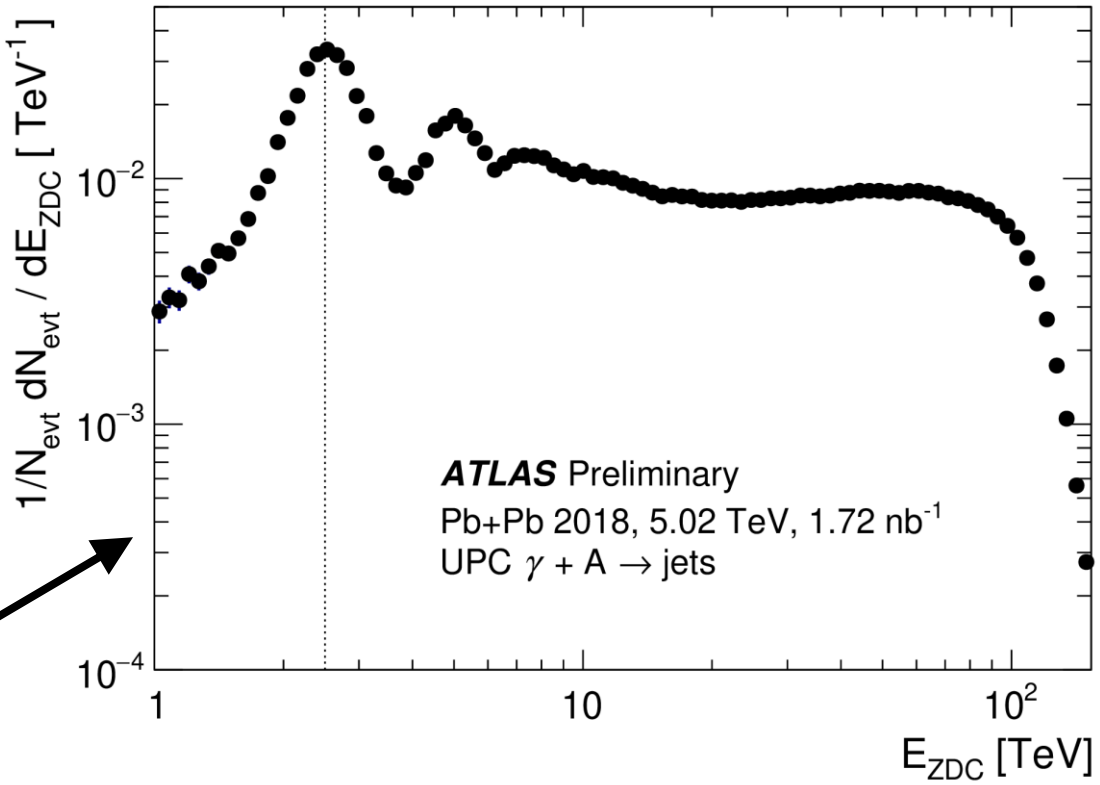

Introduction: Photo-nuclear Processes

- Large rapidity gaps are required on one side of the detector.
  - This side is dictated by the 0nXn requirement.

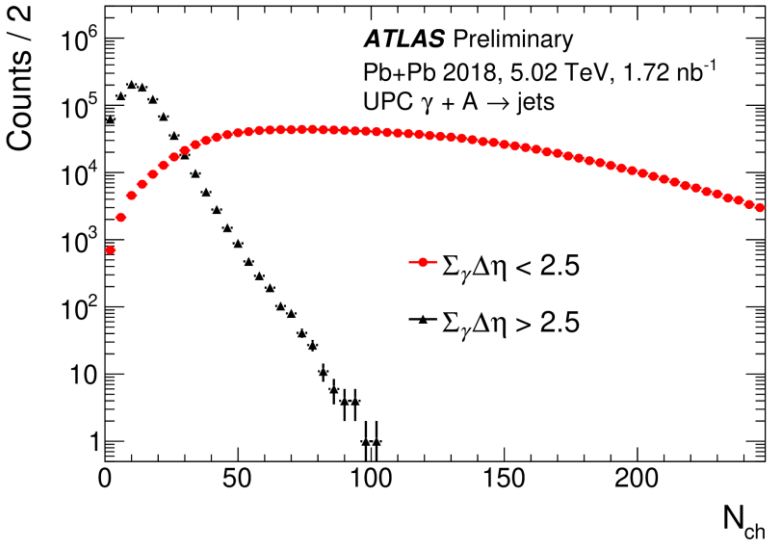

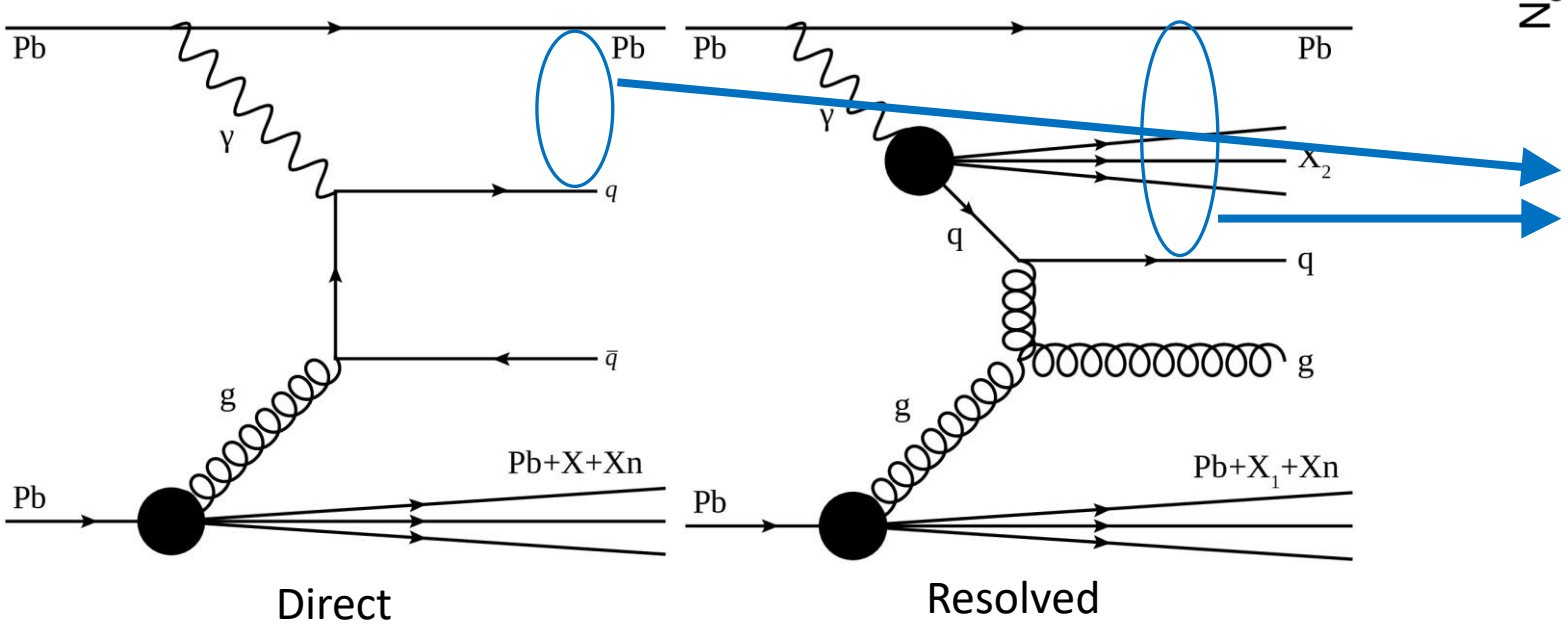

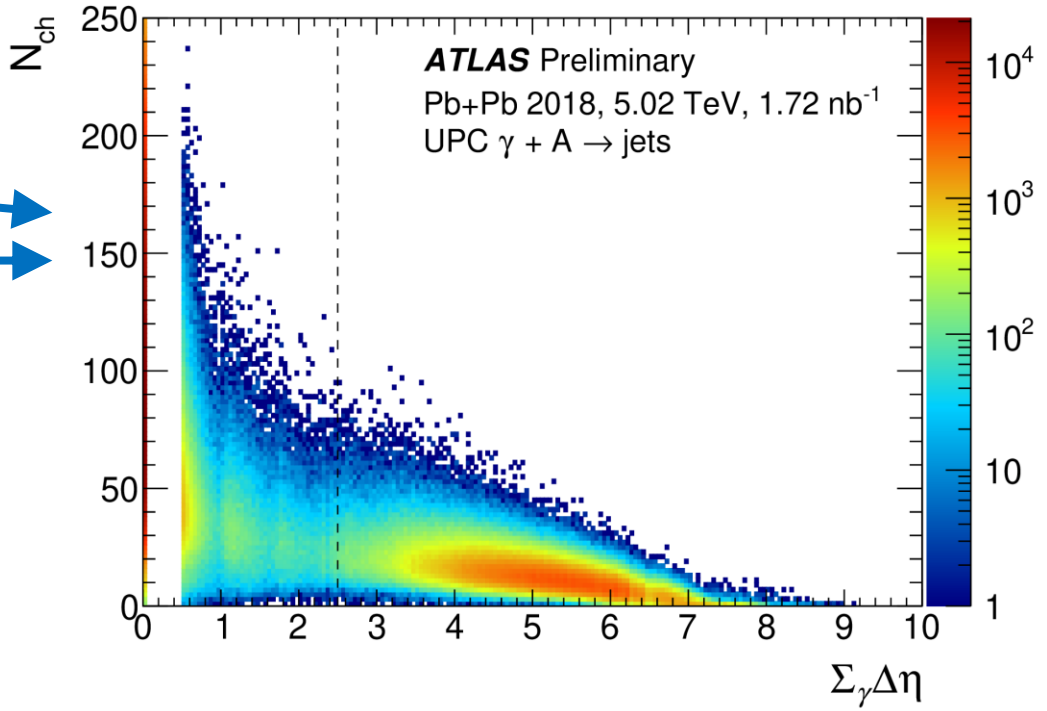

Introduction: Photo-nuclear Processes

- Large rapidity gaps are required on one side of the detector.
  - This side is dictated by the 0nXn requirement.
- This cut clearly separates out the hadronic multiplicity distribution from the photo-nuclear.

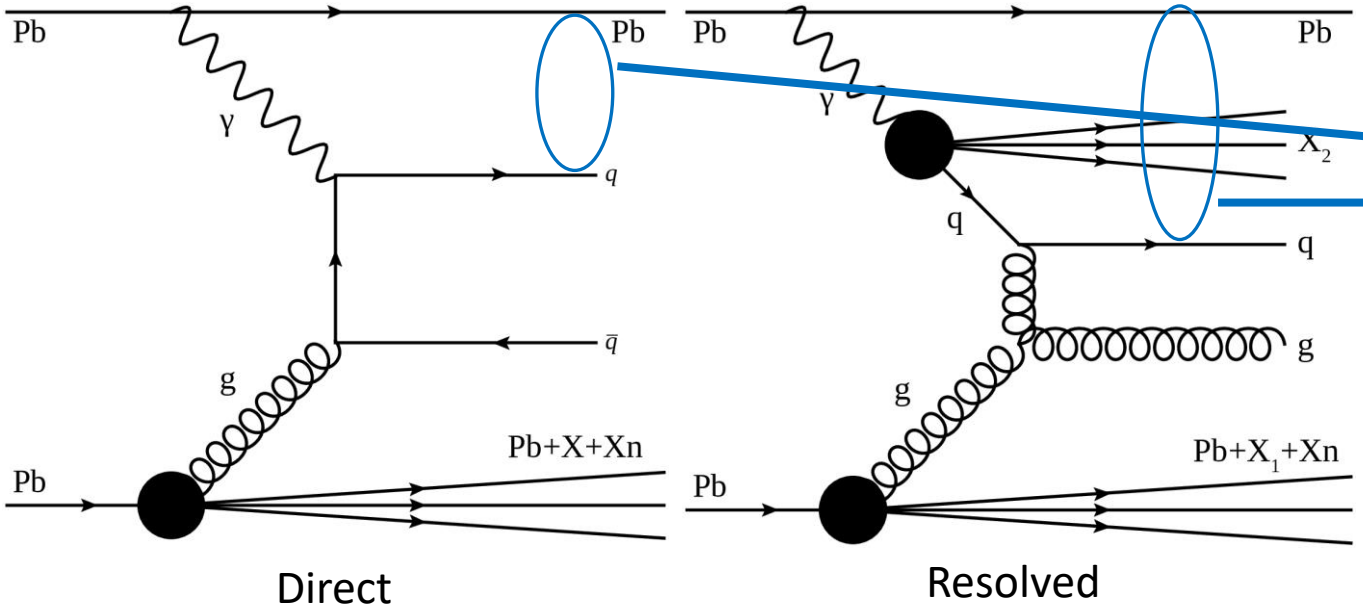

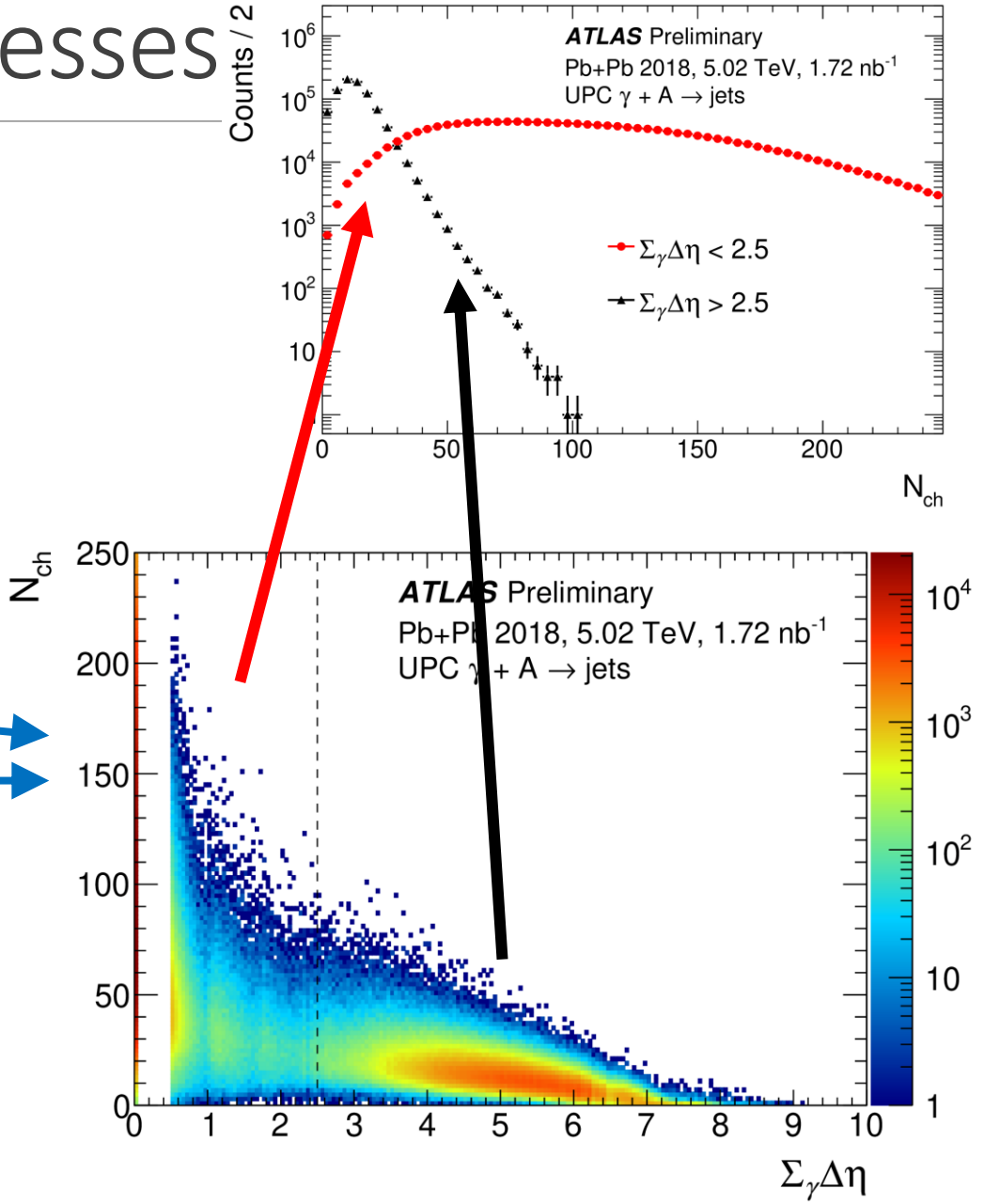

Photo-nuclear Event Topologies

- Photo-nuclear events are highly asymmetric and have a steeply falling multiplicity distribution.
  - The dN/dη distribution has not been studied before.
  - None of the MC generators shown can perfectly capture these distributions.

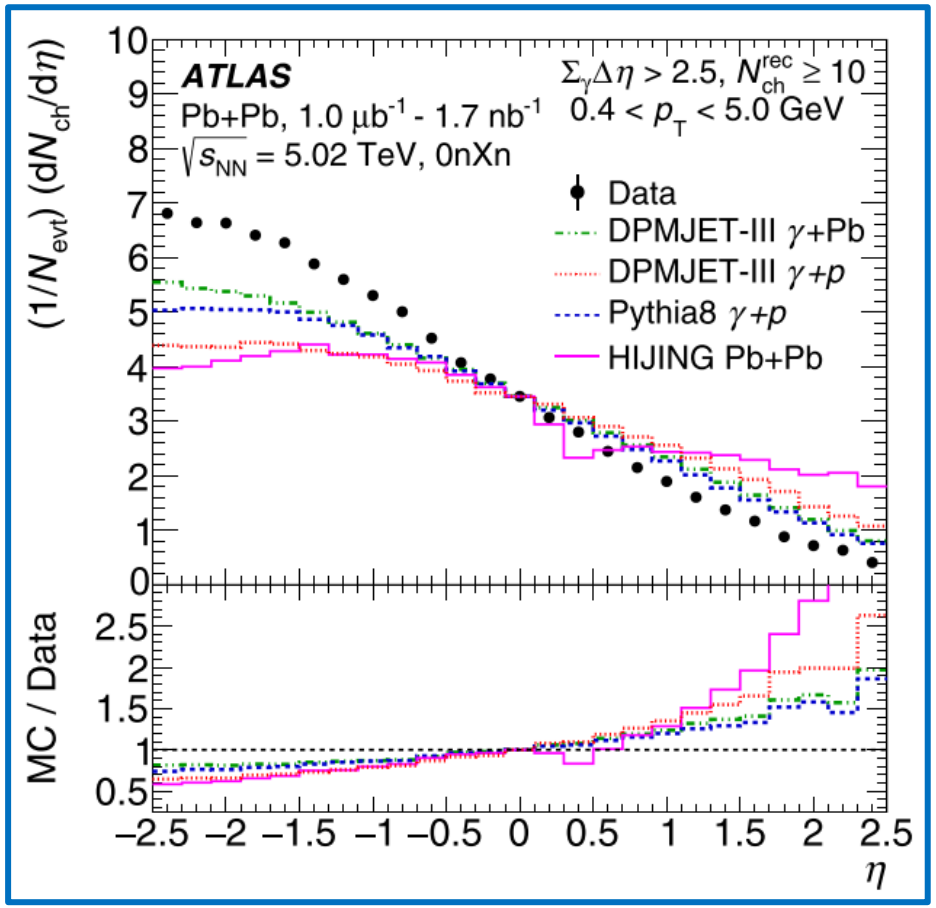

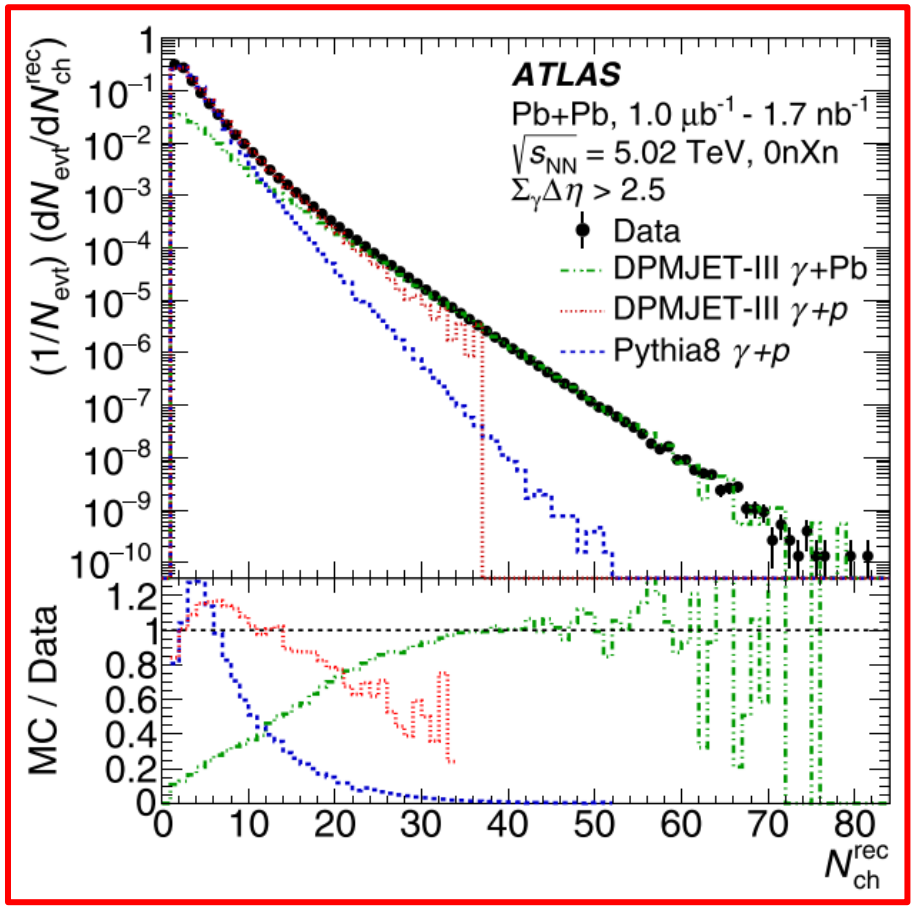

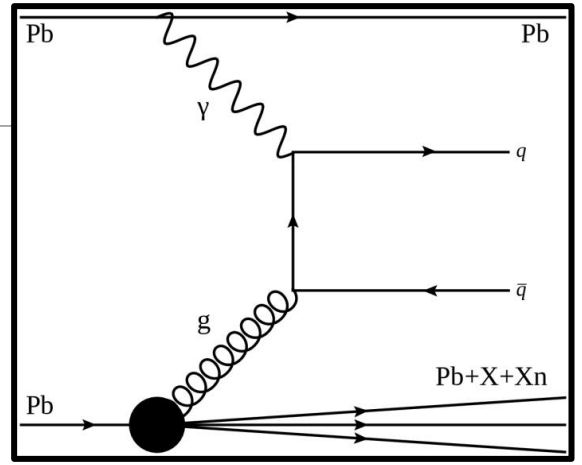

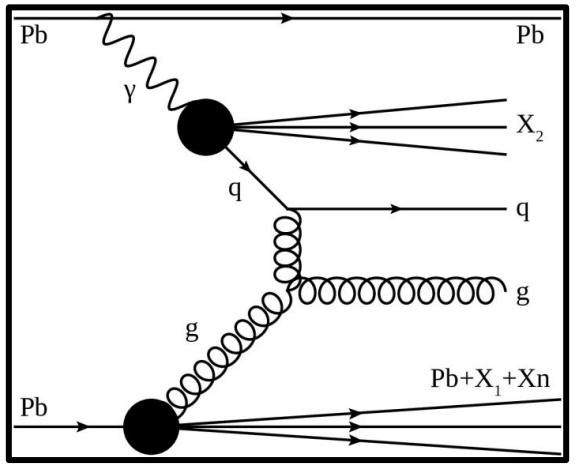

Photo-nuclear Event Topologies

- Photo-nuclear events are highly asymmetric and have a steeply falling multiplicity distribution.
  - The d
  - None

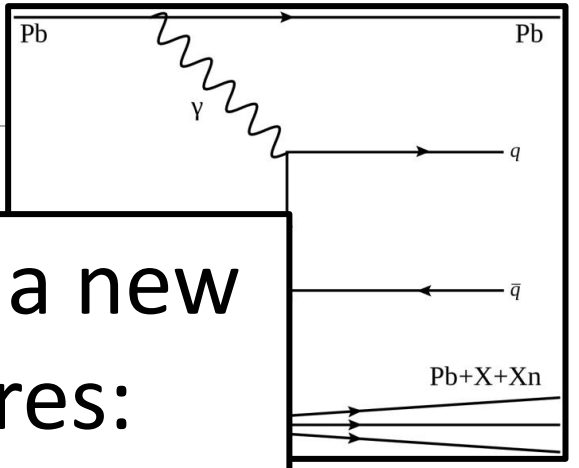

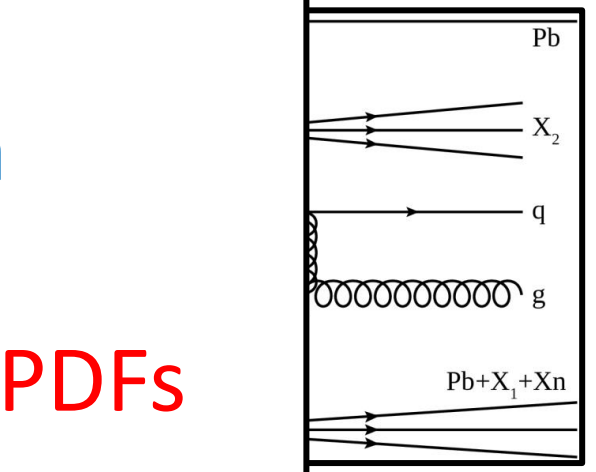

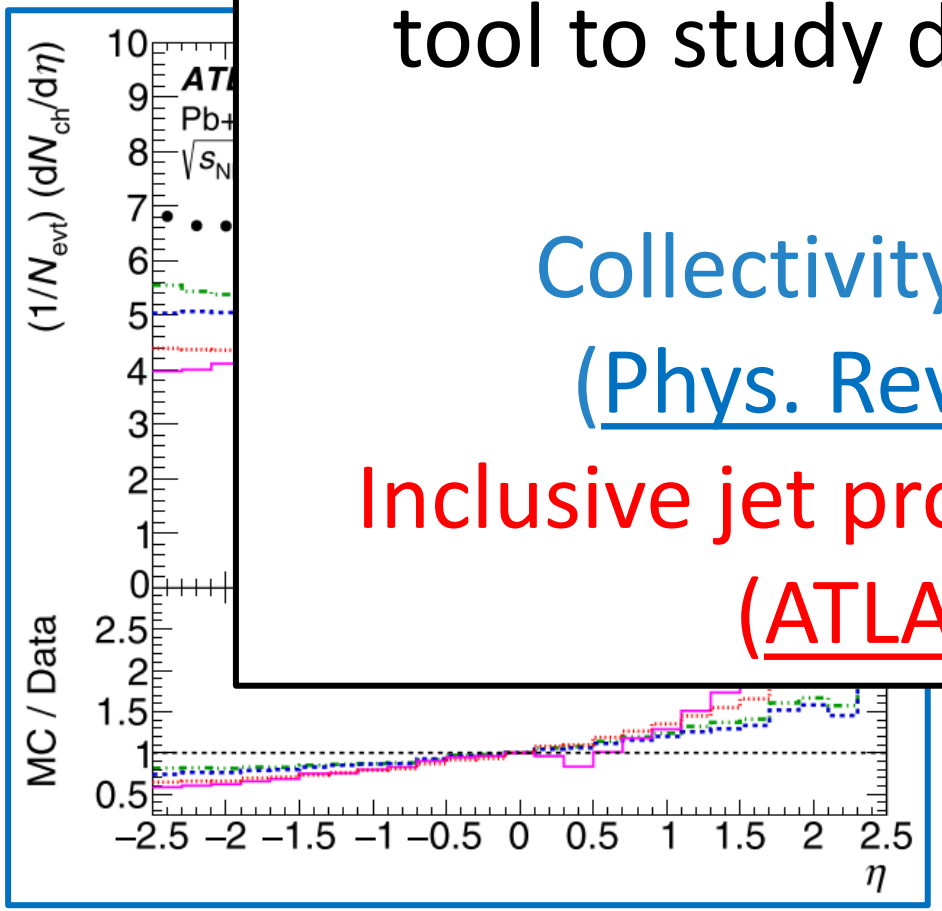

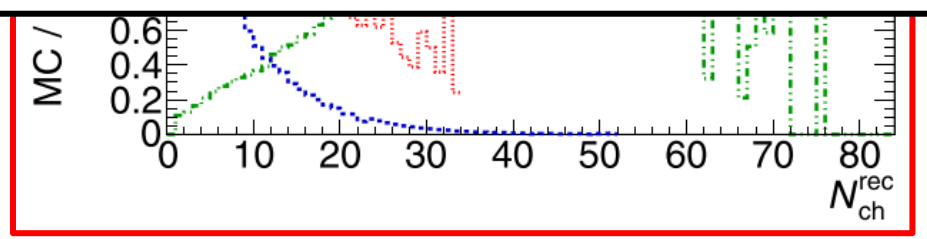

Photo-nuclear processes in UPCs provide a new tool to study different physical signatures:

Collectivity in a novel small system (Phys. Rev. C 104 (2021) 014903)

Inclusive jet production as a probe of nPDFs (ATLAS-CONF-2022-021)

Constructing Two-Particle Correlations

$$Y(\Delta\phi, \Delta\eta) = \frac{1}{N_a} \frac{d^2 N_{\text{pair}}}{d\Delta\phi\, d\Delta\eta}$$

- Yields are constructed as a function of $\Delta\eta$ and $\Delta\phi$ for charged particle tracks.

Constructing Two-Particle Correlations

$$Y(\Delta\phi, \Delta\eta) = \frac{1}{N_a} \frac{d^2 N_{\text{pair}}}{d\Delta\phi\, d\Delta\eta} \Rightarrow Y(\Delta\phi) = \int_{|\Delta\eta|=2.0}^{|\Delta\eta|=5.0} Y(\Delta\phi, |\Delta\eta|)\, d|\Delta\eta|$$

- Yields are constructed as a function of $\Delta\eta$ and $\Delta\phi$ for charged particle tracks.
- The yields in $\Delta\phi$ are determined by integrating over pairs with large $|\Delta\eta|$.
- A template for the non-flow subtraction is derived from low-multiplicity (LM) photo-nuclear data.

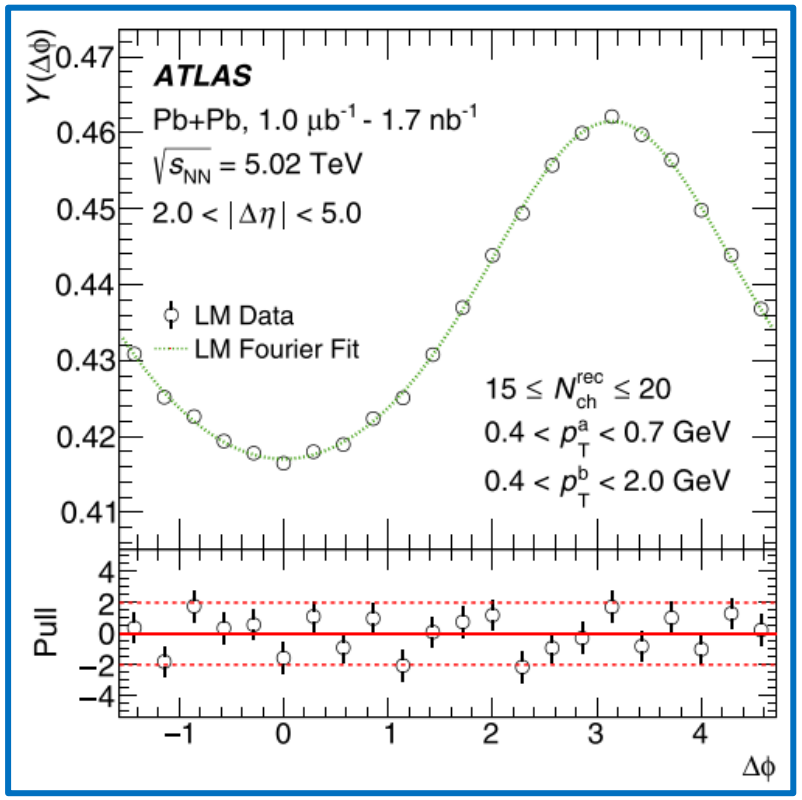

Constructing Two-Particle Correlations

$$Y(\Delta\phi, \Delta\eta) = \frac{1}{N_a}\frac{d^2N_{\text{pair}}}{d\Delta\phi\, d\Delta\eta} \Rightarrow Y(\Delta\phi) = \int_{|\Delta\eta|=2.0}^{|\Delta\eta|=5.0} Y(\Delta\phi, |\Delta\eta|)\, d|\Delta\eta| \Rightarrow$$

$$Y^{\text{HM}}(\Delta\phi) = FY^{\text{LM}}(\Delta\phi) + G\left\{1 + 2\sum_{n=2}^{4} v_{n,n}\cos(n\Delta\phi)\right\}$$
$$= FY^{\text{LM}}(\Delta\phi) + Y^{\text{ridge}}(\Delta\phi)$$

- Yields are constructed as a function of $\Delta\eta$ and $\Delta\phi$ for charged particle tracks.
- The yields in $\Delta\phi$ are determined by integrating over pairs with large $|\Delta\eta|$.
- A template for the non-flow subtraction is derived from low-multiplicity (LM) photo-nuclear data.
- Template fits to high-multiplicity (HM) data allow us to extract the yield not explained by LM non-flow contribution.

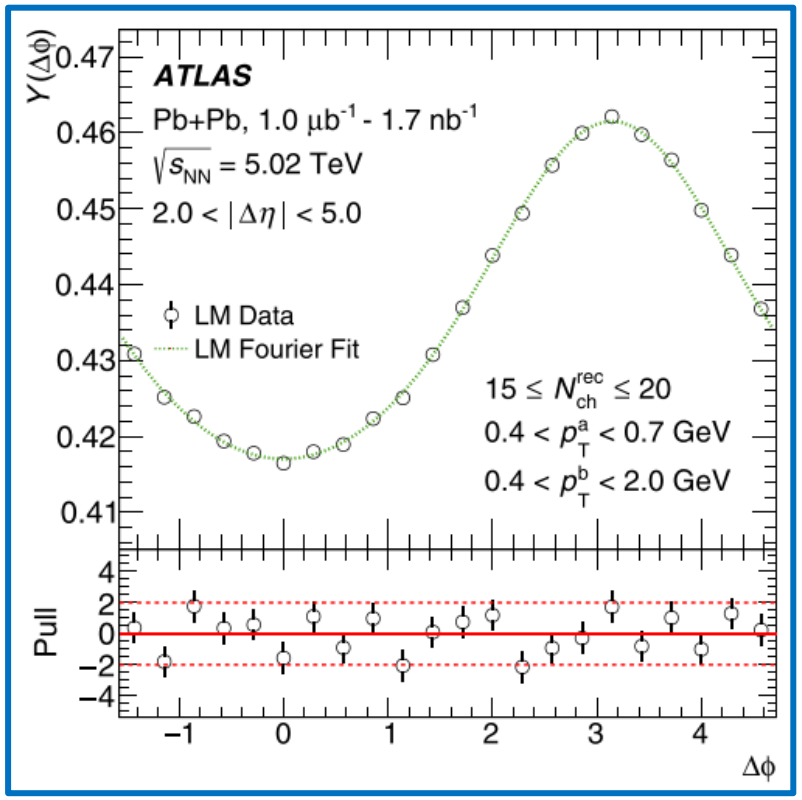

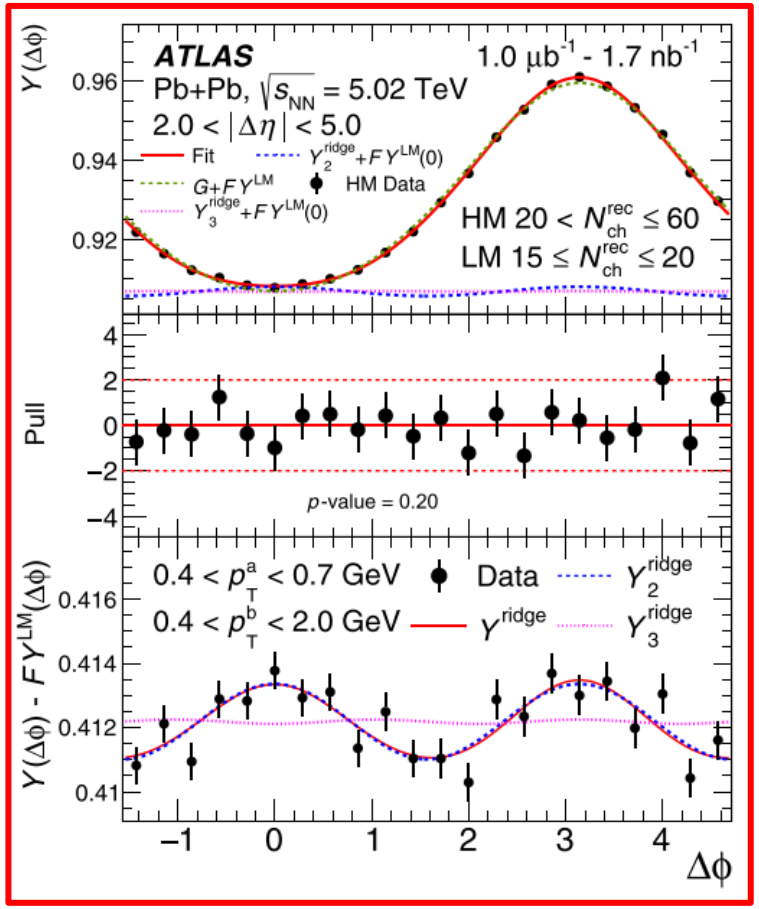

Multiplicity-Dependence of Correlations

- Applying this procedure for extracting the flow coefficients allows them to be compared to *pp* and *pPb* with similar multiplicity.
  - The flow signal in photonuclear collisions is smaller than in pp but clearly significant.

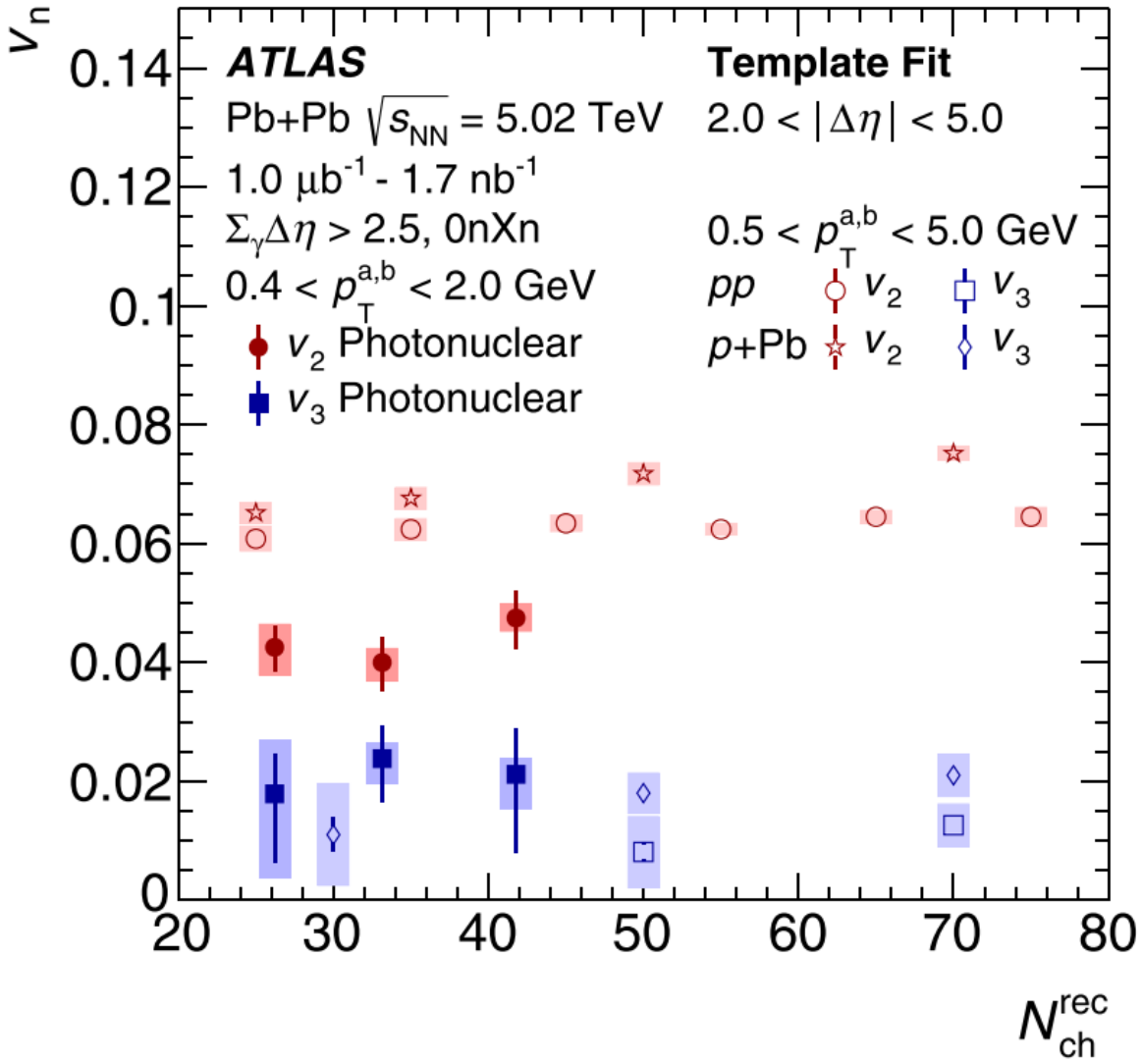

p_T-Dependence of Correlations

- Applying this procedure for extracting the flow coefficients allows them to be compared to *pp* and *pPb* with similar multiplicity.
  - The flow signal in photonuclear collisions is smaller than in pp but clearly significant.
- The v_2 also demonstrates a p_T-dependence characteristic of hydrodynamic expansion.

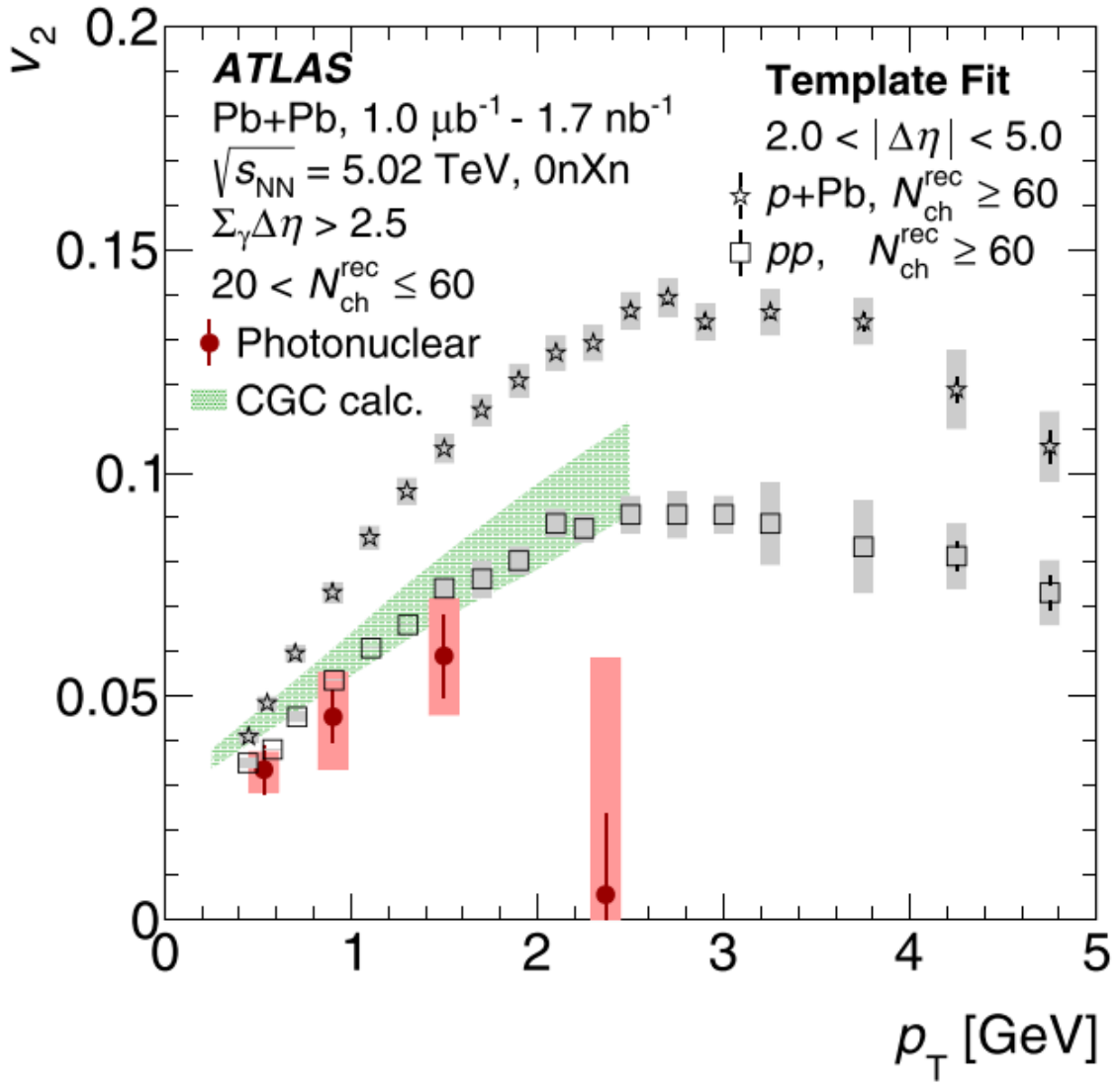

Interpreting UPC Correlations

- In the Vector Meson Dominance (VMD) model, the resolved photon can be treated as a rho-nucleus collision.
- This model with (3+1)D hydrodynamic evolution (right) can effectively reproduce the ATLAS data for $v_2(p_T)$.

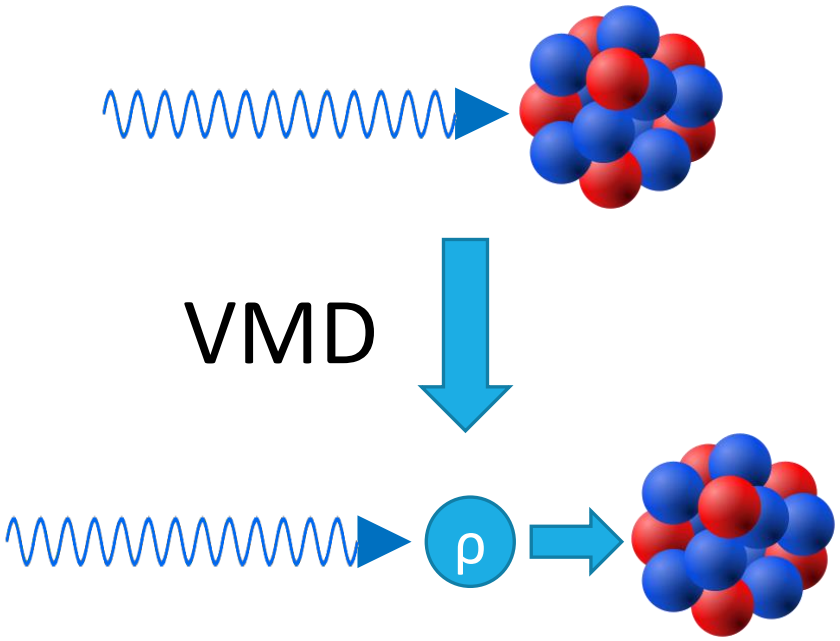

Zhao, Shen, and Schenke, nucl-th/2203.06094

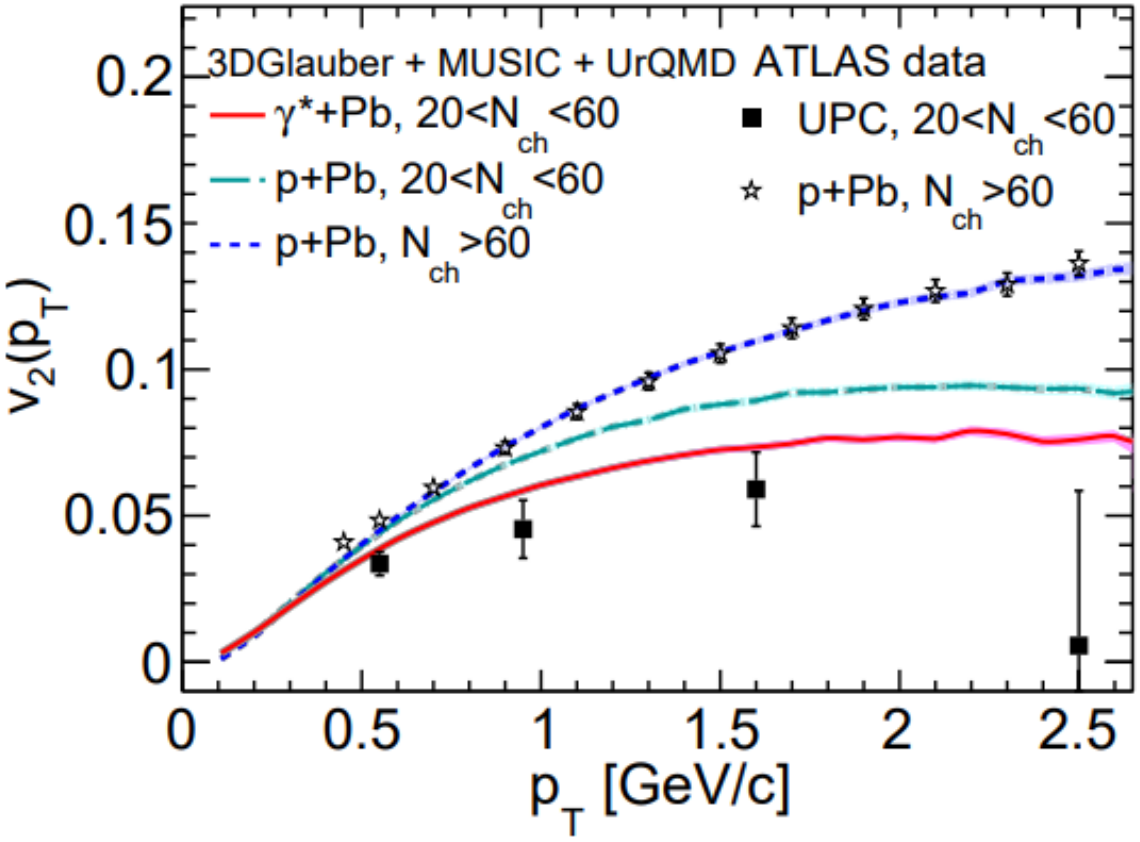

Photo-nuclear Dijet Events

- If we add a jet selection, we can reconstruct the hard-scattering kinematics.
  - We add a requirement for 2 offline Particle-Flow jets.
  - Jets are required to have p_T > 15 GeV.

$$H_T \equiv \sum_i p_T^i$$

$$x_A \equiv \frac{M_{jets} e^{-y_{jets}}}{\sqrt{s_{NN}}}$$

$$z_\gamma \equiv \frac{M_{jets} e^{+y_{jets}}}{\sqrt{s_{NN}}}$$

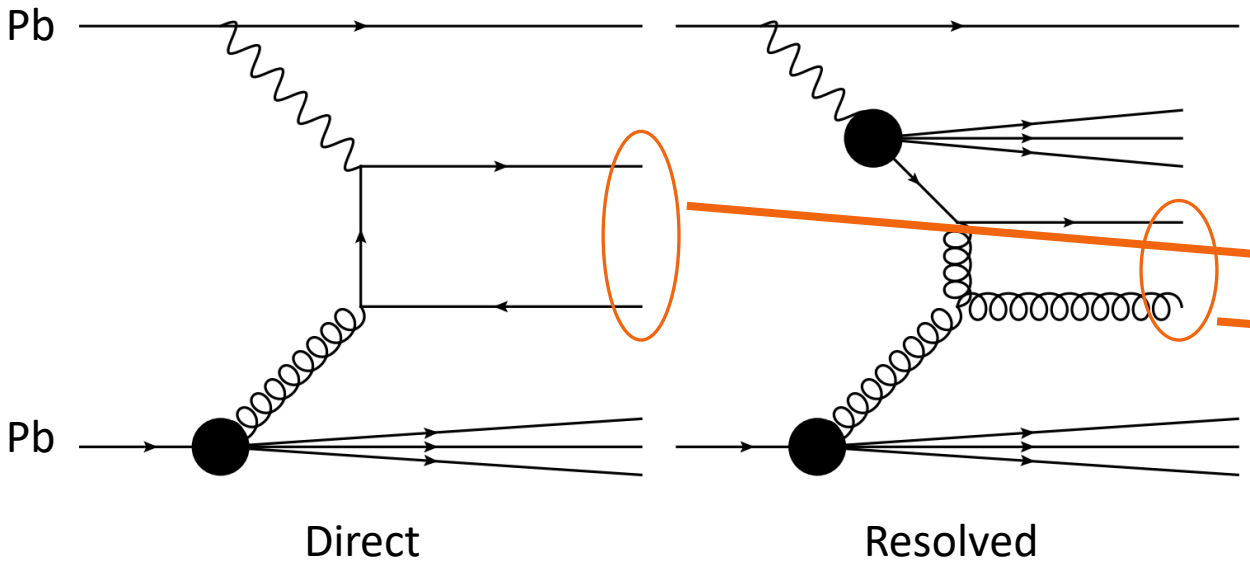

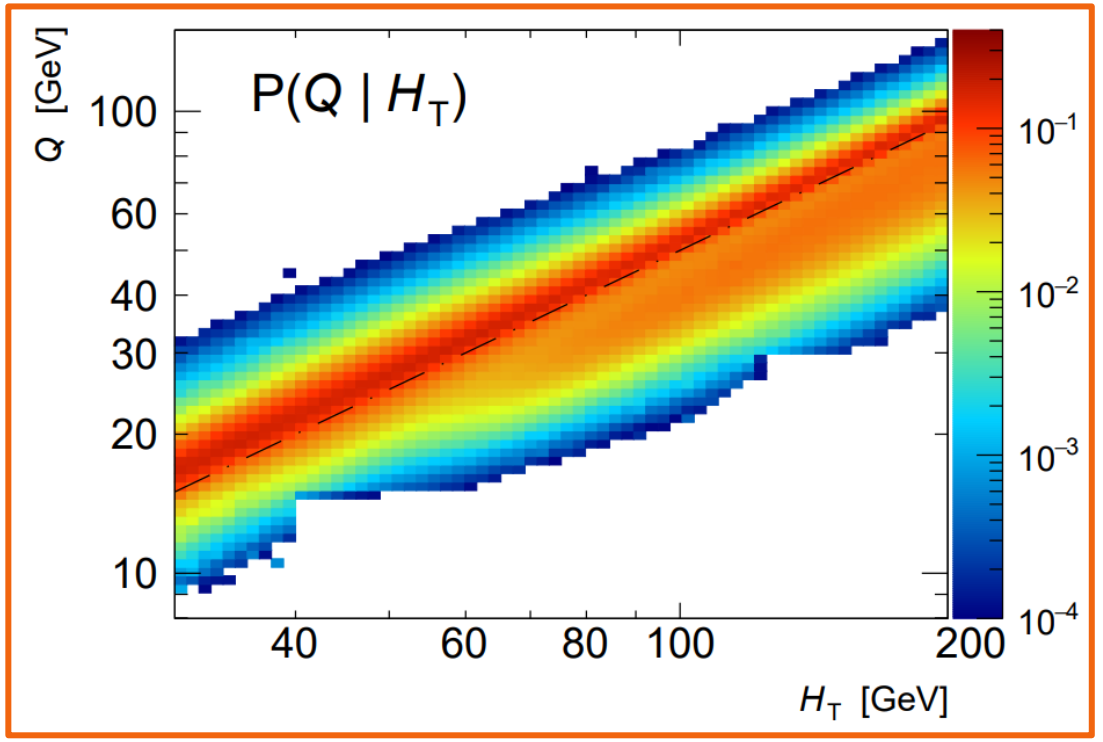

Jet kinematics provide access to the hard-scattering kinematics, directly probing nuclear PDF effects.

$H_T \sim 2Q$ $\quad$ $x_A \sim x$

Photo-nuclear Dijet Events

- If we add a jet selection, we can reconstruct the hard-scattering kinematics.
  - We add a requirement for 2 offline Particle-Flow jets.
  - Jets are required to have p_T > 15 GeV.

$$H_T \equiv \sum_i p_T^i$$

$$x_A \equiv \frac{M_{jets} e^{-y_{jets}}}{\sqrt{s_{NN}}}$$

$$z_\gamma \equiv \frac{M_{jets} e^{+y_{jets}}}{\sqrt{s_{NN}}}$$

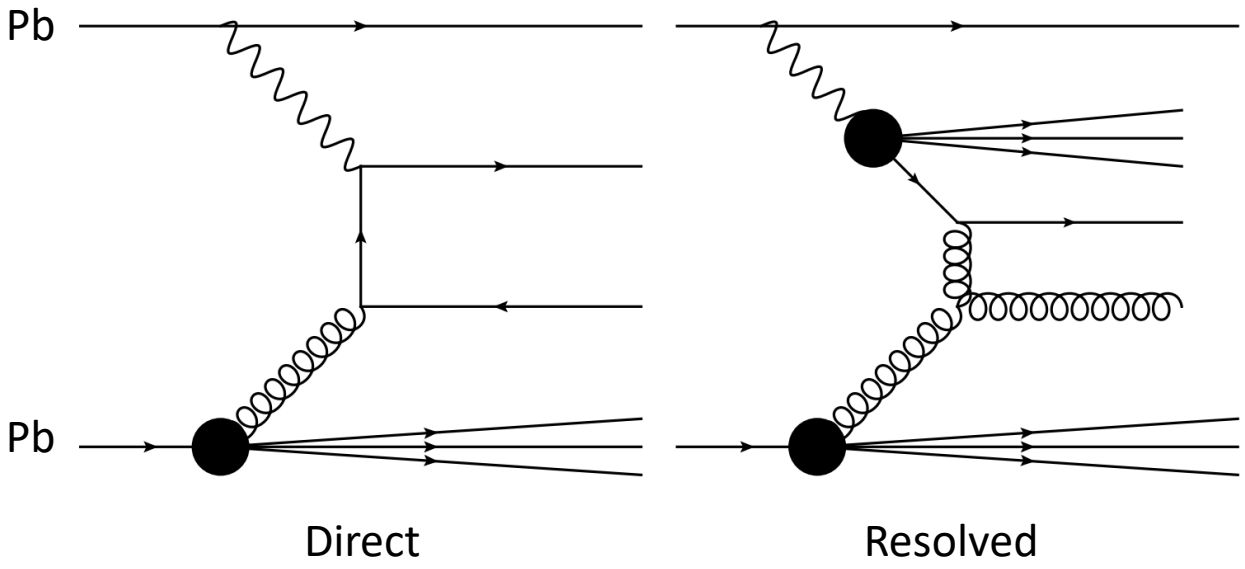

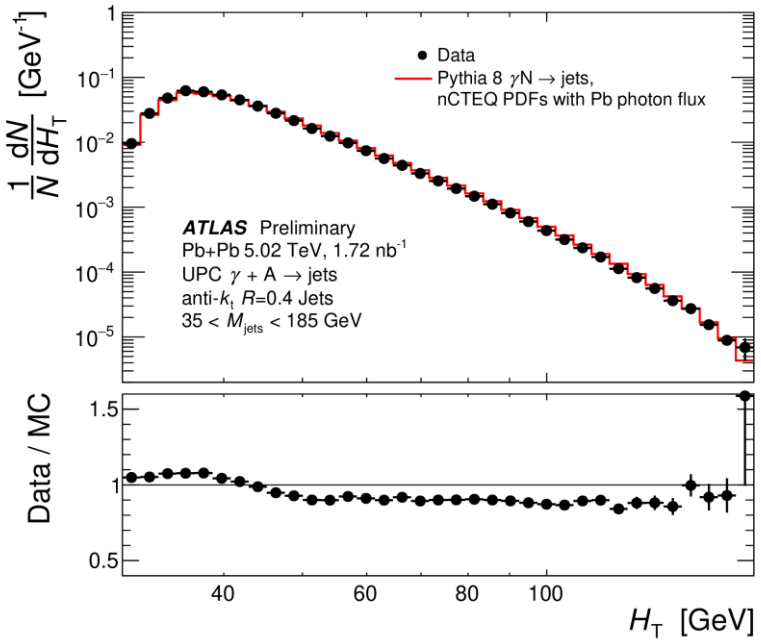

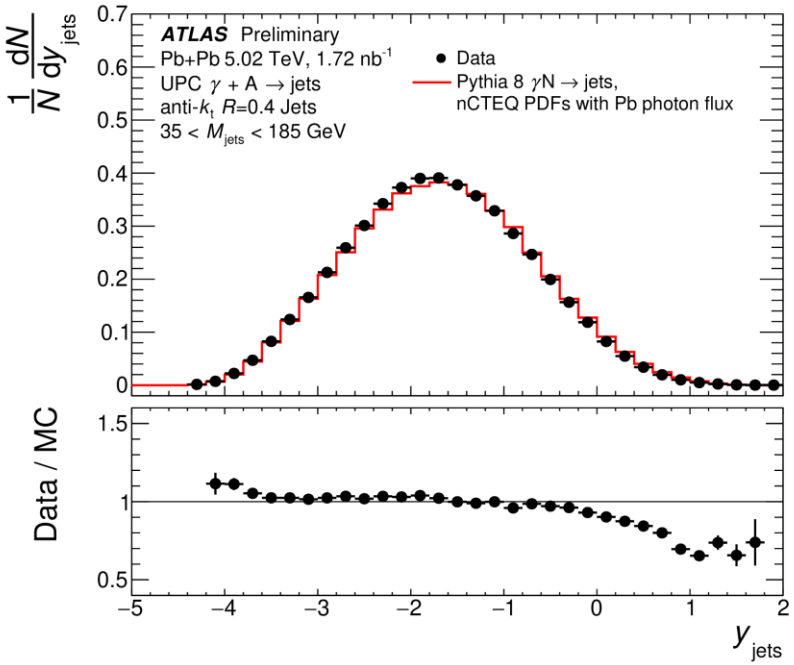

Photo-nuclear Dijet Events

- If we add a jet selection, we can reconstruct the hard-scattering kinematics.
  - We add a requirement for 2 offline Particle-Flow jets.
  - Jets are required to have p_T > 15 GeV.

$$H_T \equiv \sum_i p_T^i$$

$$x_A \equiv \frac{M_{jets} e^{-y_{jets}}}{\sqrt{s_{NN}}}$$

$$z_\gamma \equiv \frac{M_{jets} e^{+y_{jets}}}{\sqrt{s_{NN}}}$$

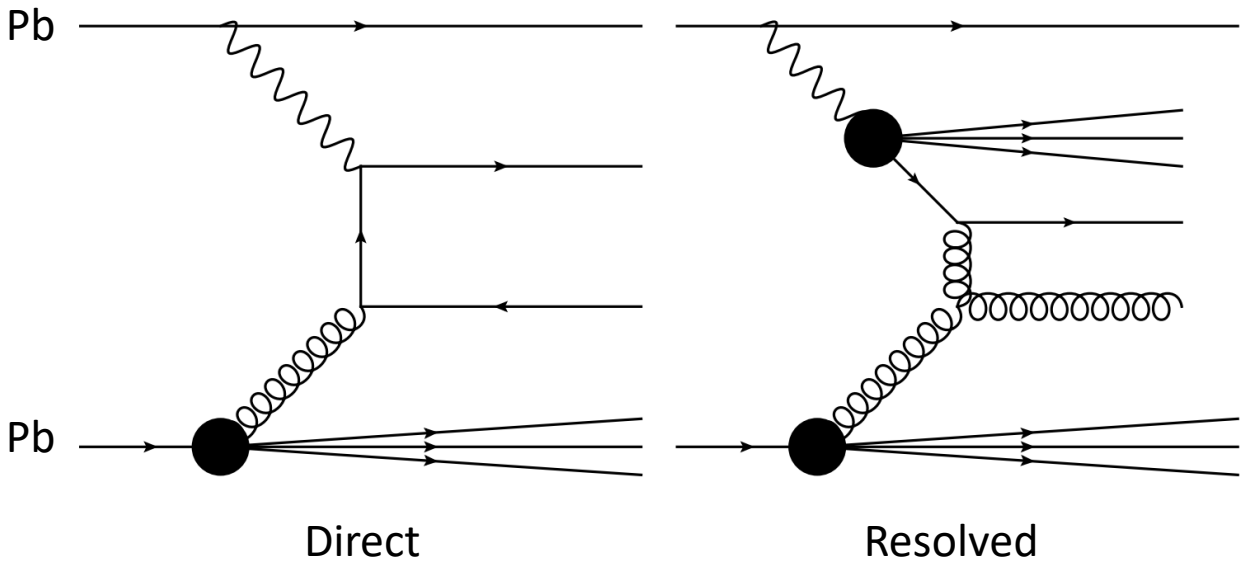

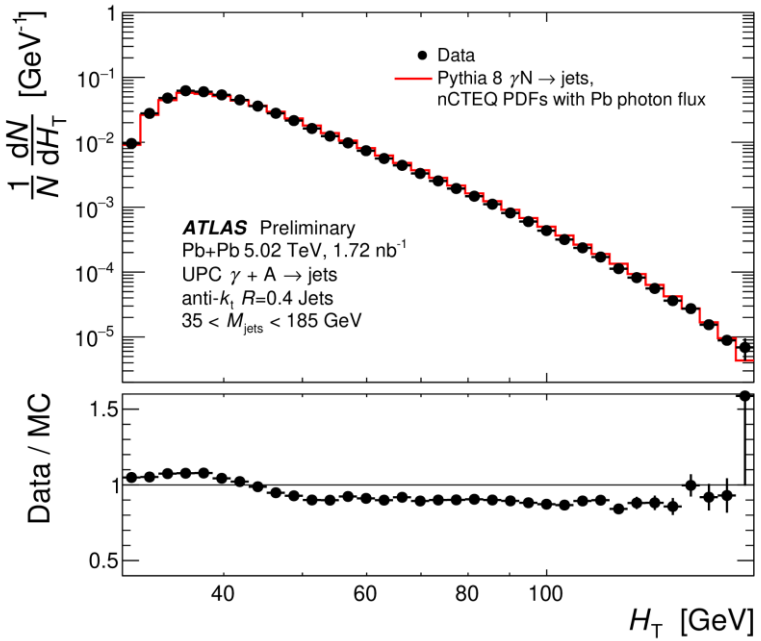

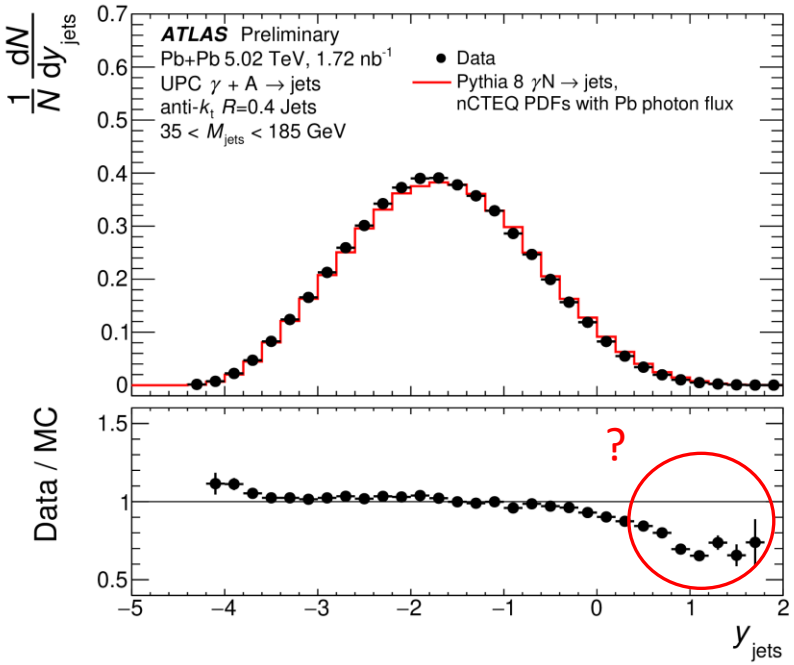

The Measured Photon Flux

- Breakup of the photon-emitting nucleus is a substantial effect, both in data estimates and theoretical modelling.
  - All model comparisons shown are corrected with the "Theory" points.

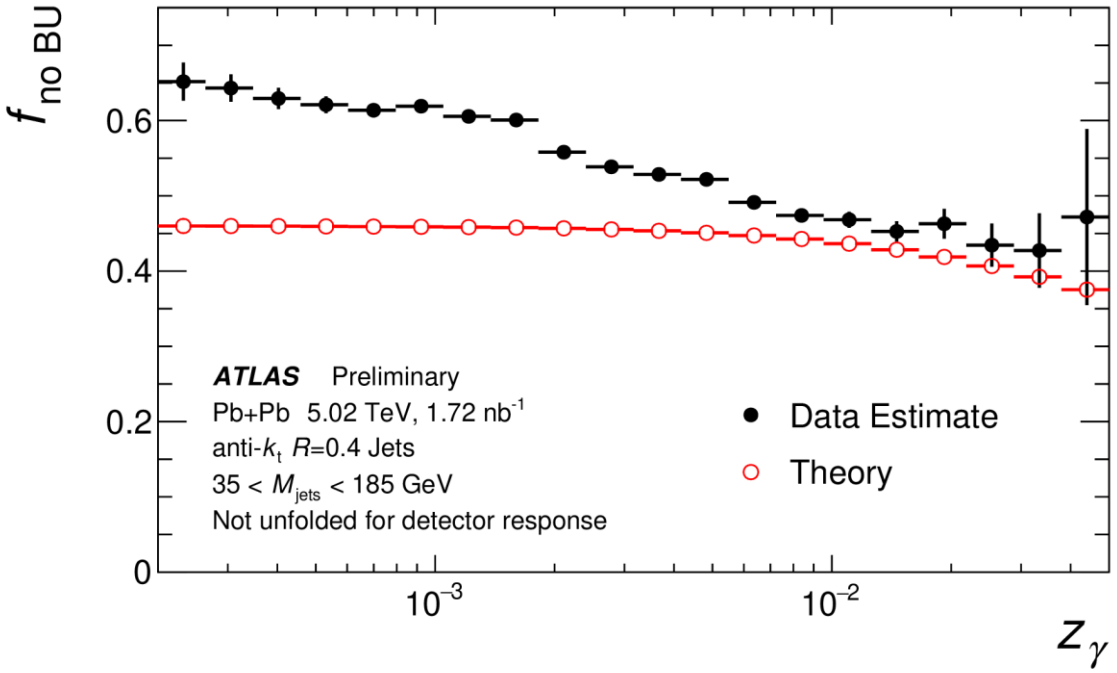

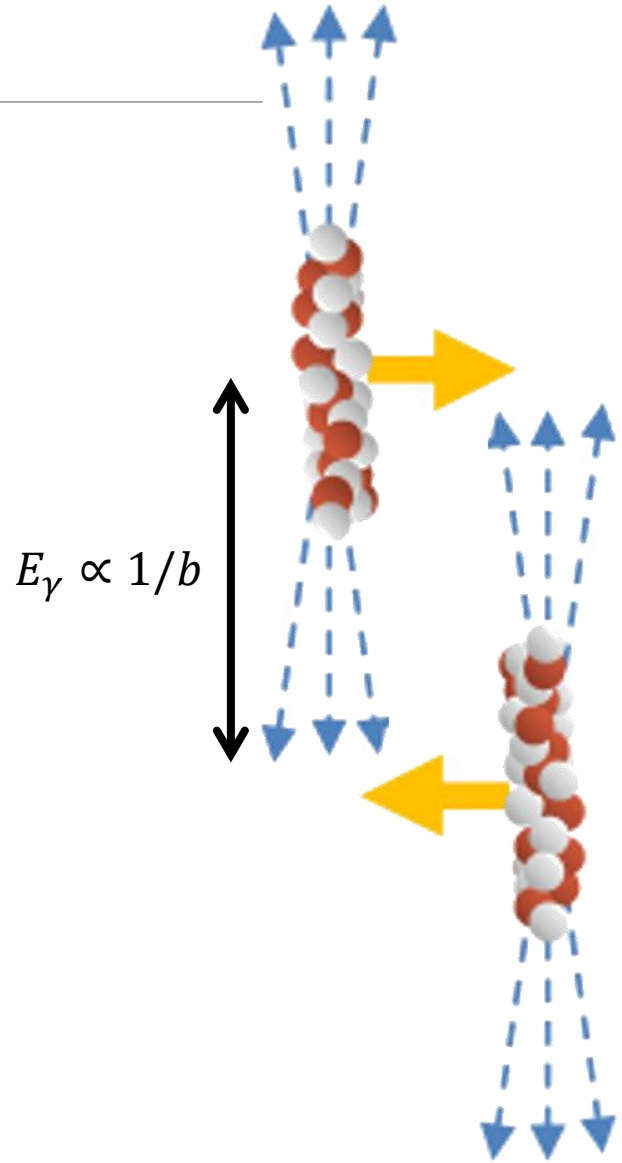

The Measured Photon Flux

- Breakup of the photon-emitting nucleus is a substantial effect, both in data estimates and theoretical modelling.
  - All model comparisons shown are corrected with the "Theory" points.
  - Disagreements appear to arise more at low z_γ, where the breakup model tends to over-correct.

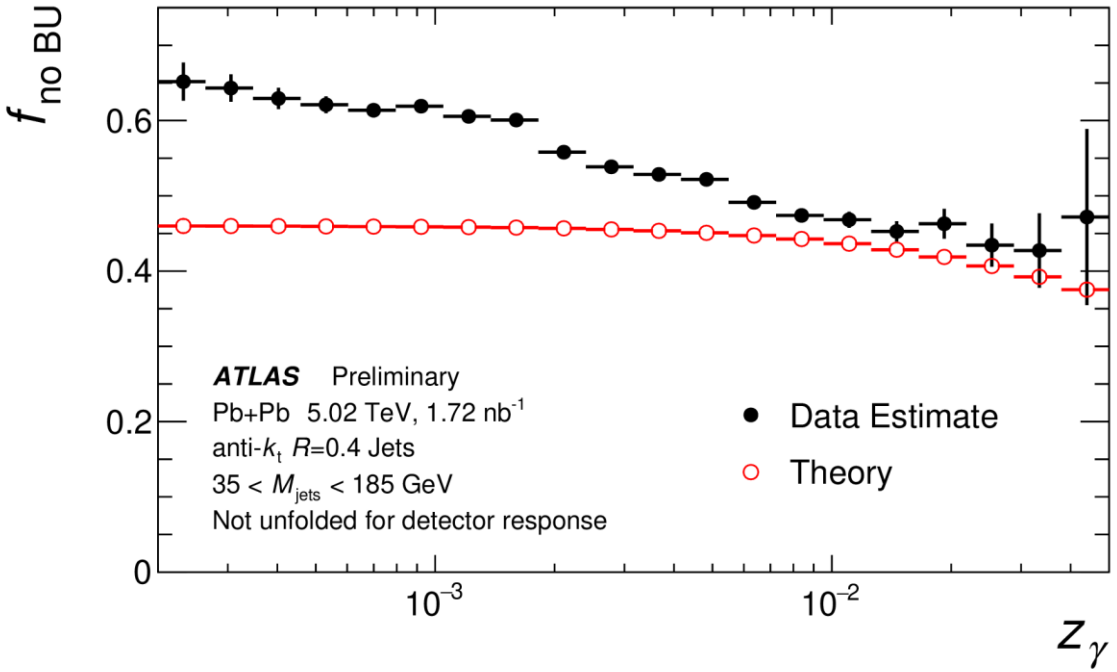

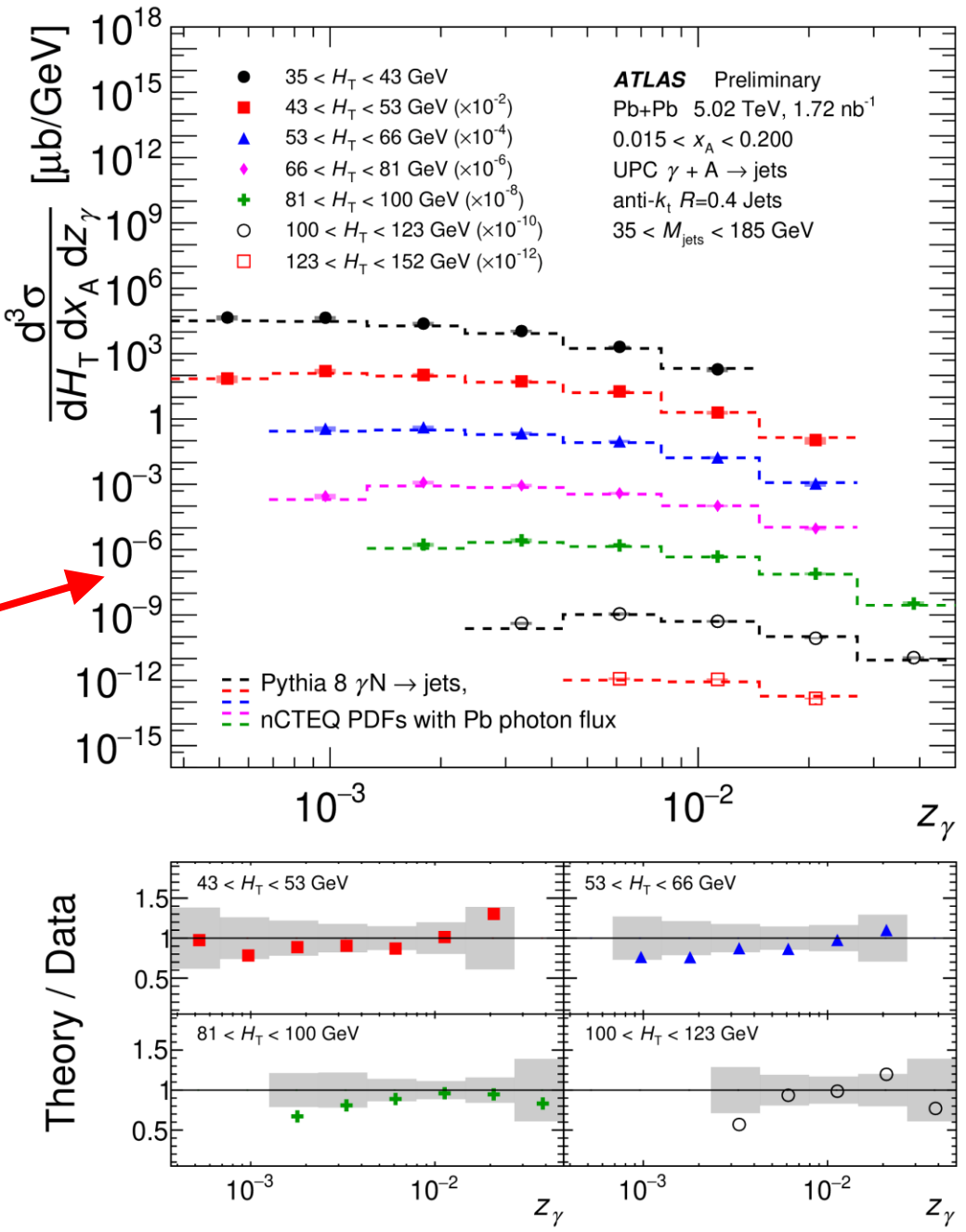

Scanning in Photon Energy

$$H_T \equiv \sum_i p_T^i \qquad x_A \equiv \frac{M_{jets} e^{-y_{jets}}}{\sqrt{s_{NN}}} \qquad z_\gamma \equiv \frac{M_{jets} e^{+y_{jets}}}{\sqrt{s_{NN}}}$$

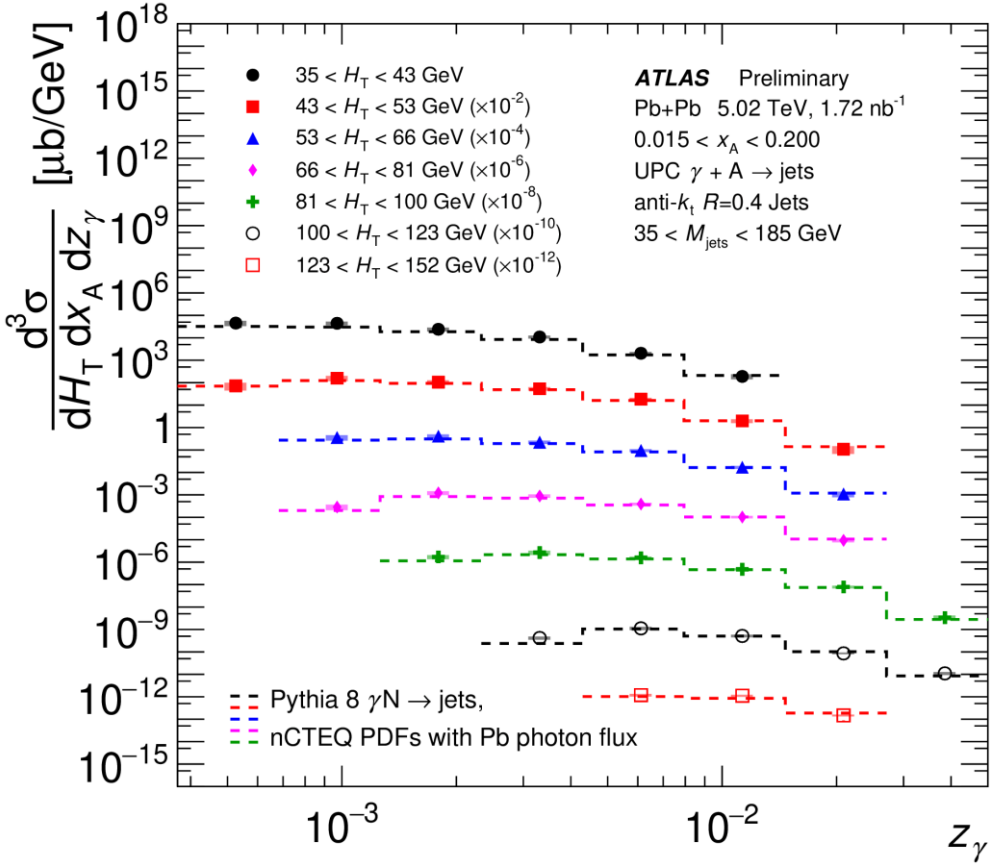

The x_A distribution has substantial acceptance effects in z_γ.

Selecting a photon energy removes this bias, allowing a more direct measurement of PDF effects.

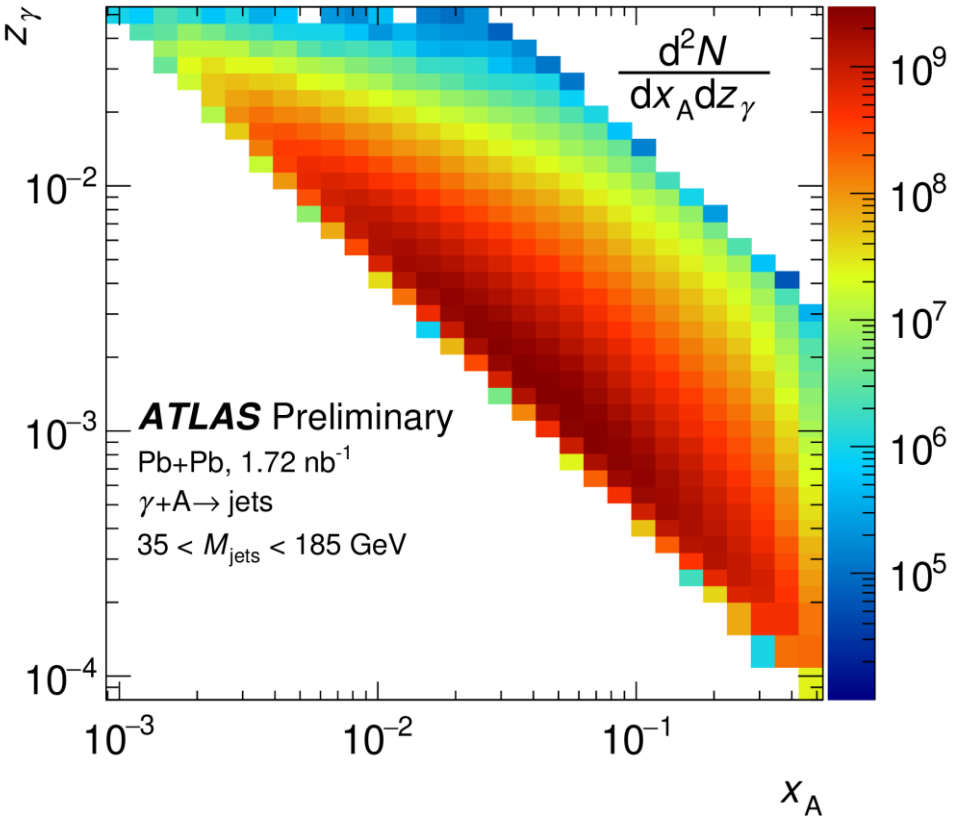

Scanning in Photon Energy

$$H_T \equiv \sum_i p_T^i \qquad x_A \equiv \frac{M_{jets} e^{-y_{jets}}}{\sqrt{s_{NN}}} \qquad z_\gamma \equiv \frac{M_{jets} e^{+y_{jets}}}{\sqrt{s_{NN}}}$$

The x_A distribution has substantial acceptance effects in z_γ.

Selecting a photon energy removes this bias, allowing a more direct measurement of PDF effects.

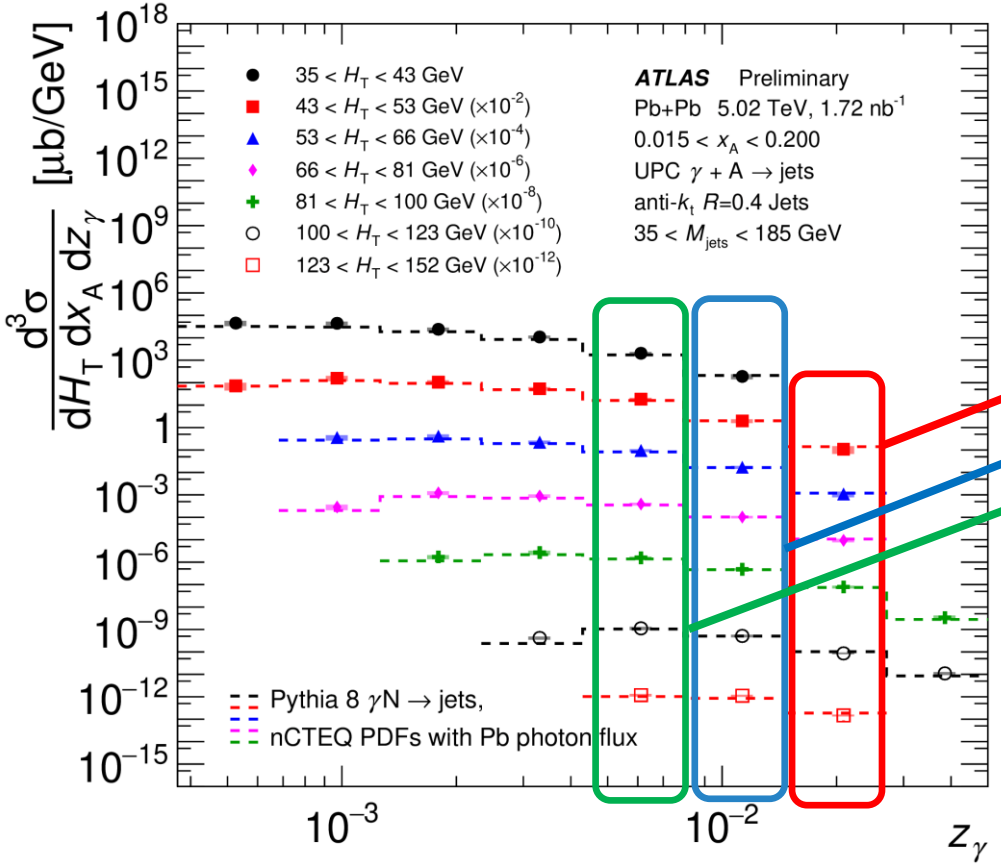

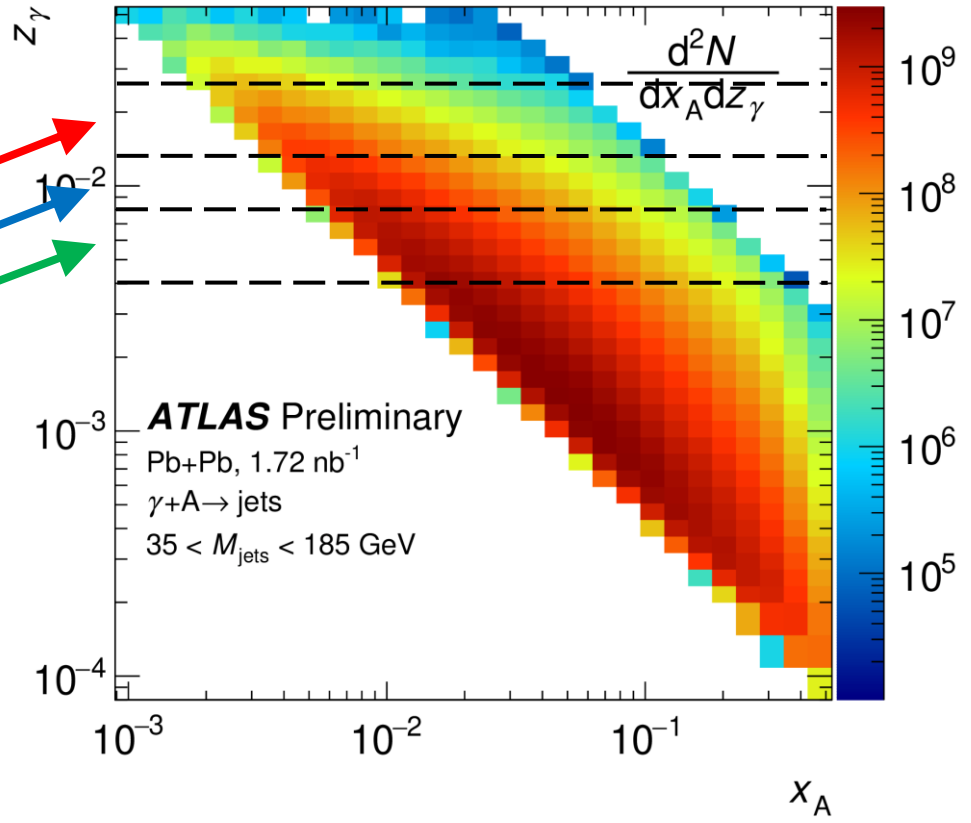

Measured Cross-Sections

- At intermediate photon energies, we can access higher-x partons.

$$H_T \equiv \sum_i p_T^i \qquad x_A \equiv \frac{M_{jets} e^{-y_{jets}}}{\sqrt{s_{NN}}} \qquad z_\gamma \equiv \frac{M_{jets} e^{+y_{jets}}}{\sqrt{s_{NN}}}$$

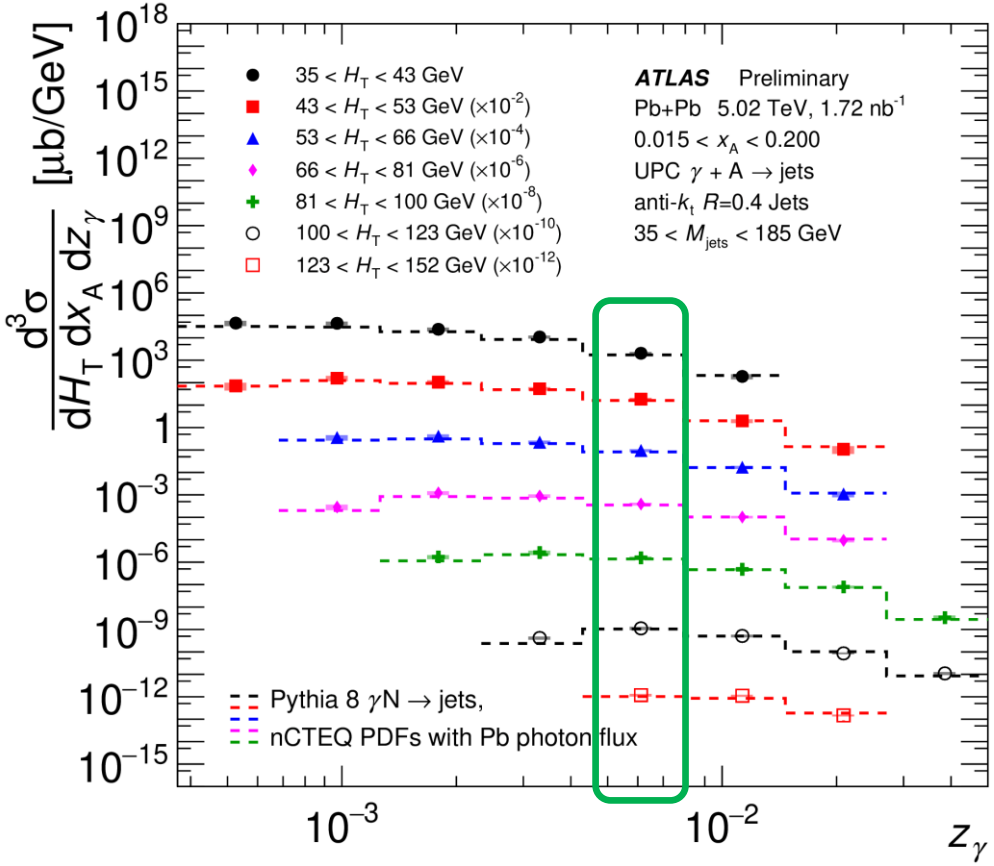

Photon Energy

$0.004 < z_\gamma < 0.008$

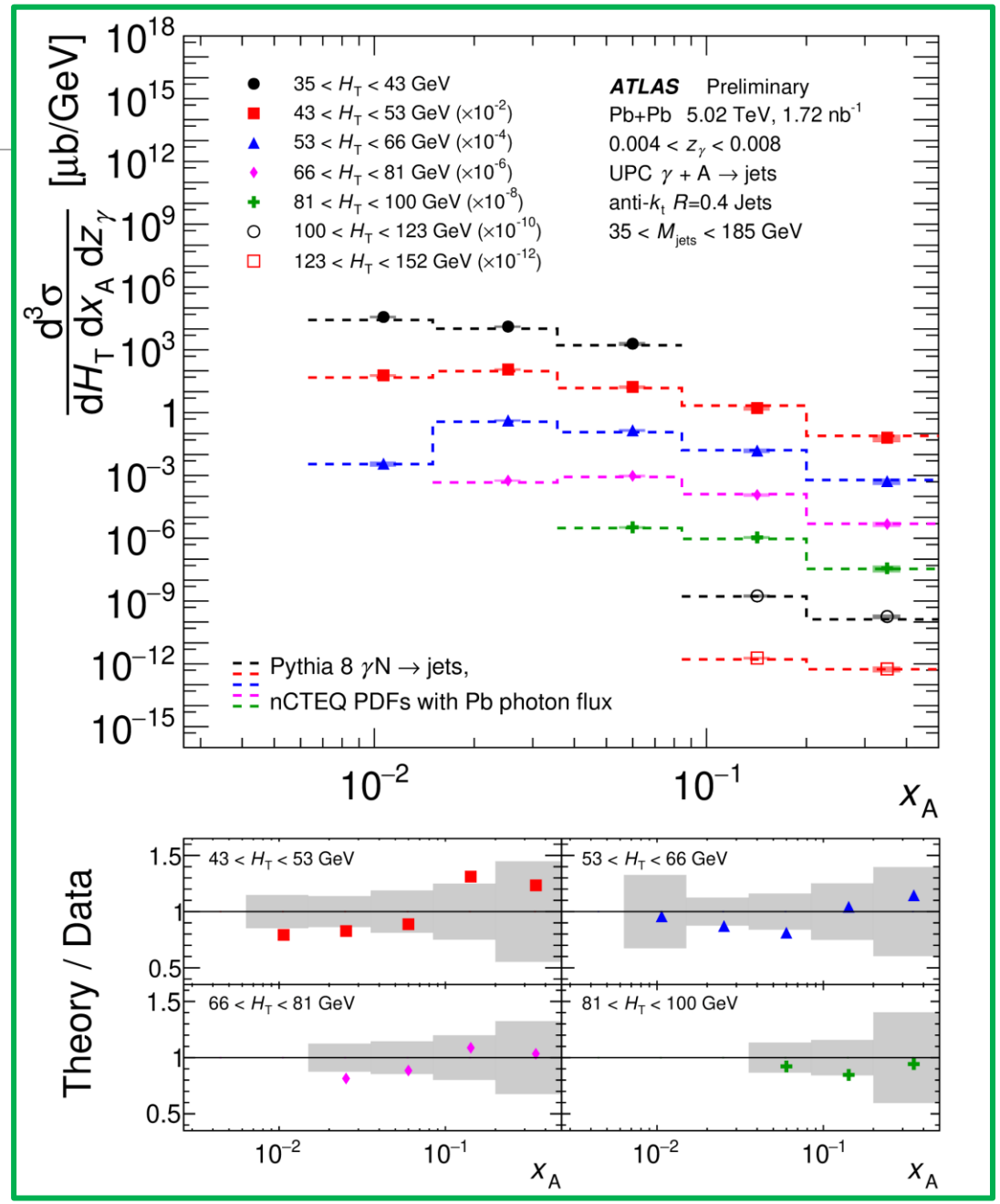

Measured Cross-Sections

- Going higher in photon energy opens up the low-x shadowing region.
- Results are quite consistent with the theoretical model.

$$H_T \equiv \sum_i p_T^i \qquad x_A \equiv \frac{M_{jets} e^{-y_{jets}}}{\sqrt{s_{NN}}} \qquad z_\gamma \equiv \frac{M_{jets} e^{+y_{jets}}}{\sqrt{s_{NN}}}$$

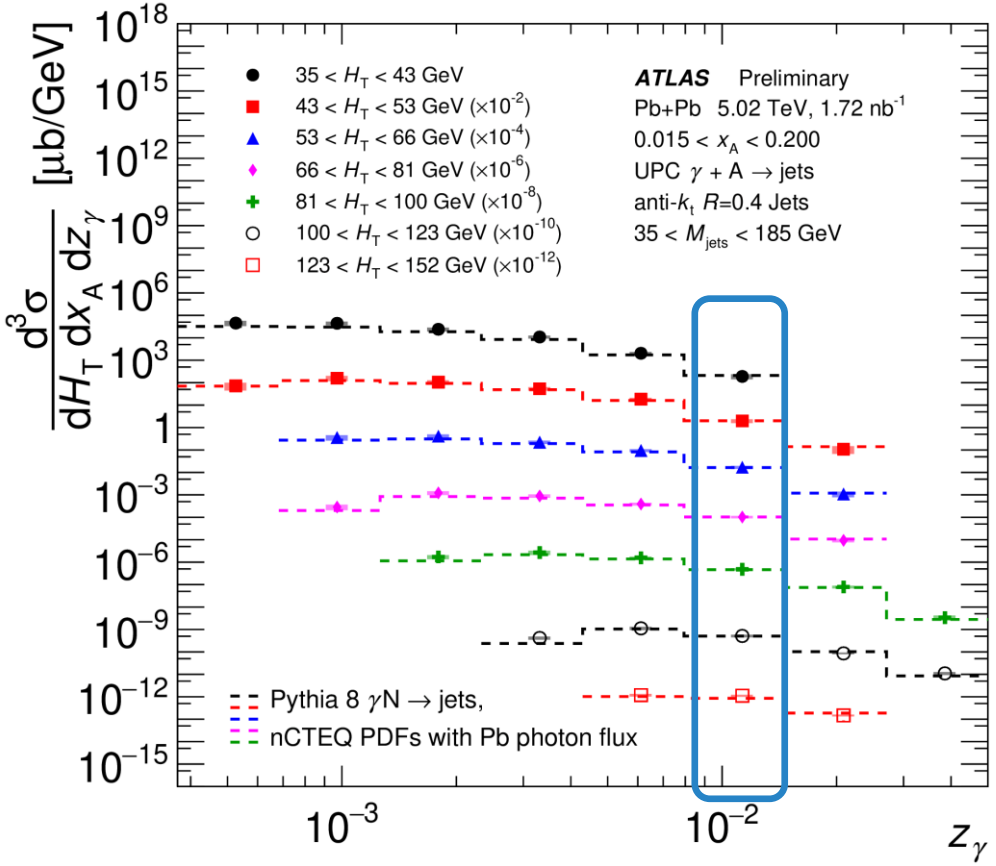

Photon Energy

$0.008 < z_\gamma < 0.015$

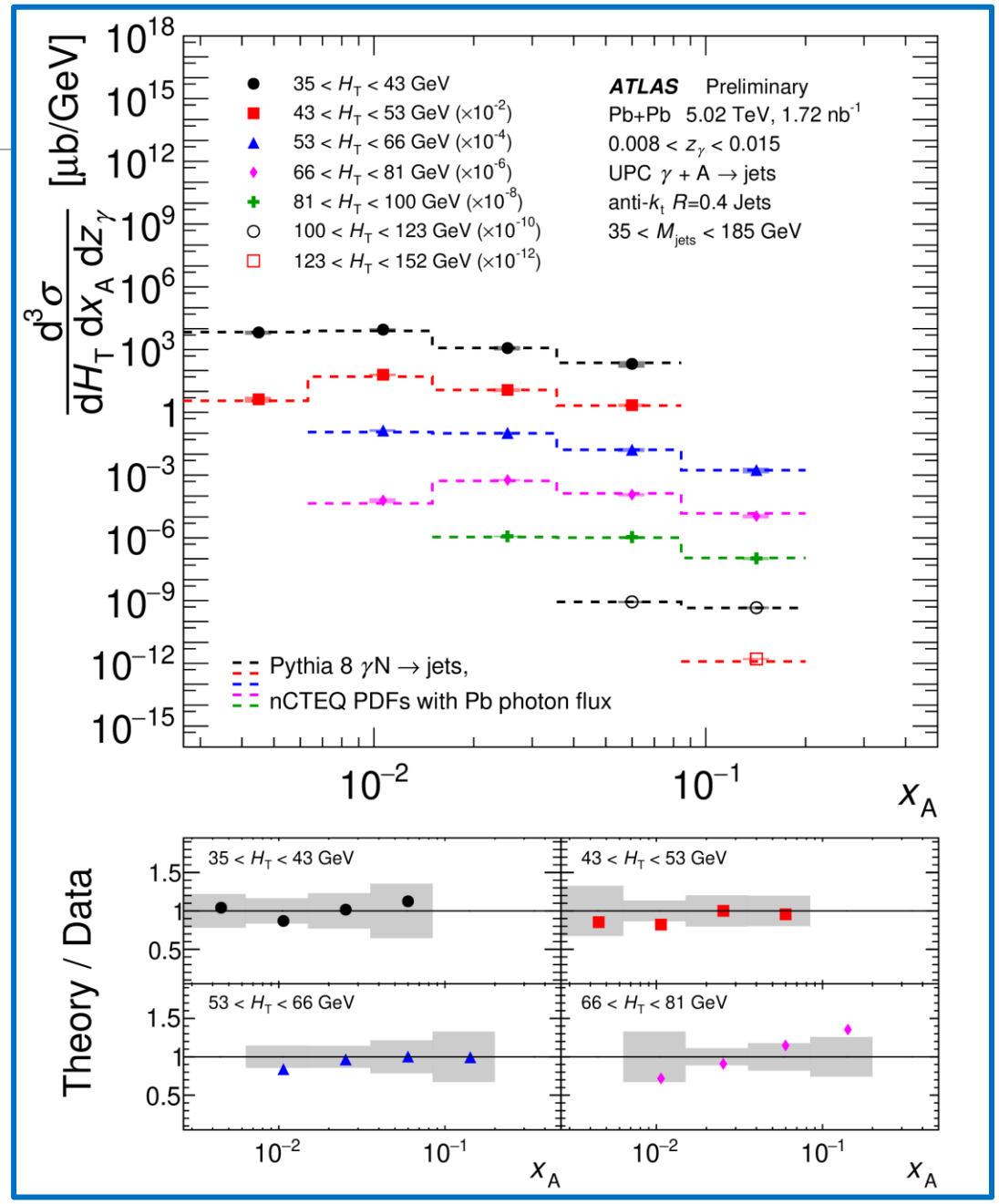

Measured Cross-Sections

- The highest photon energy allows the most access to low-x.
- Systematic control is more of a challenge near acceptance edges.

$$H_T \equiv \sum_i p_T^i \qquad x_A \equiv \frac{M_{jets} e^{-y_{jets}}}{\sqrt{s_{NN}}} \qquad z_\gamma \equiv \frac{M_{jets} e^{+y_{jets}}}{\sqrt{s_{NN}}}$$

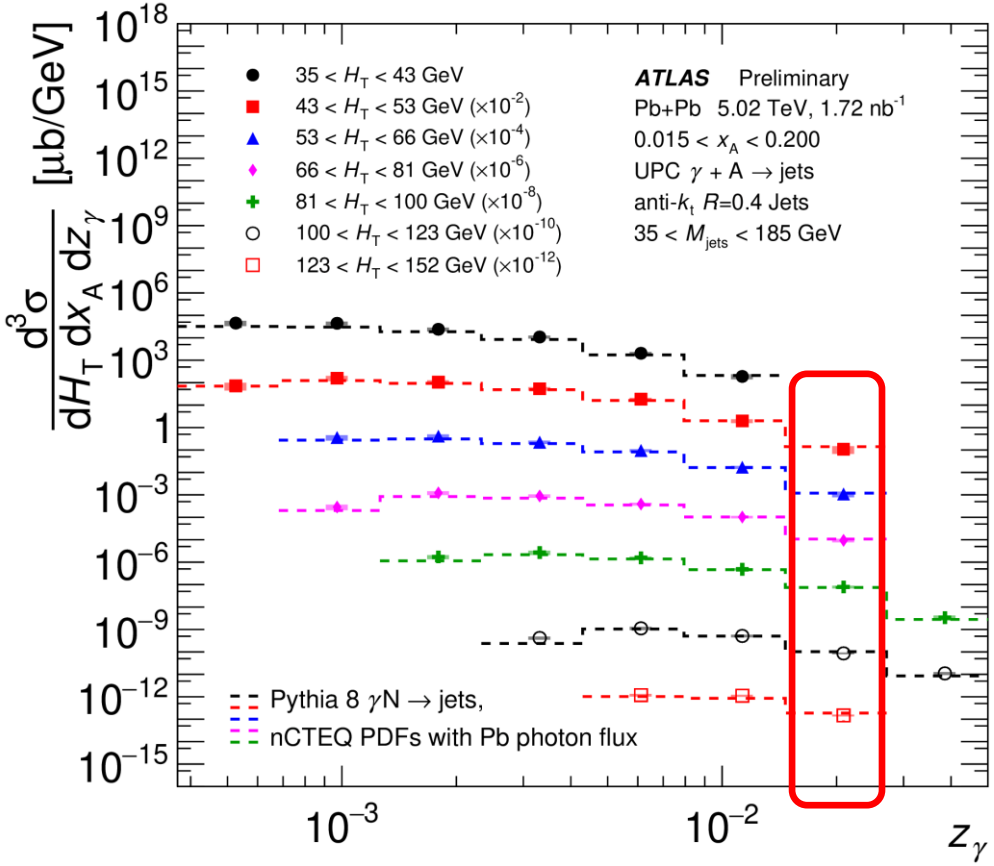

Photon Energy

$0.015 < z_\gamma < 0.027$

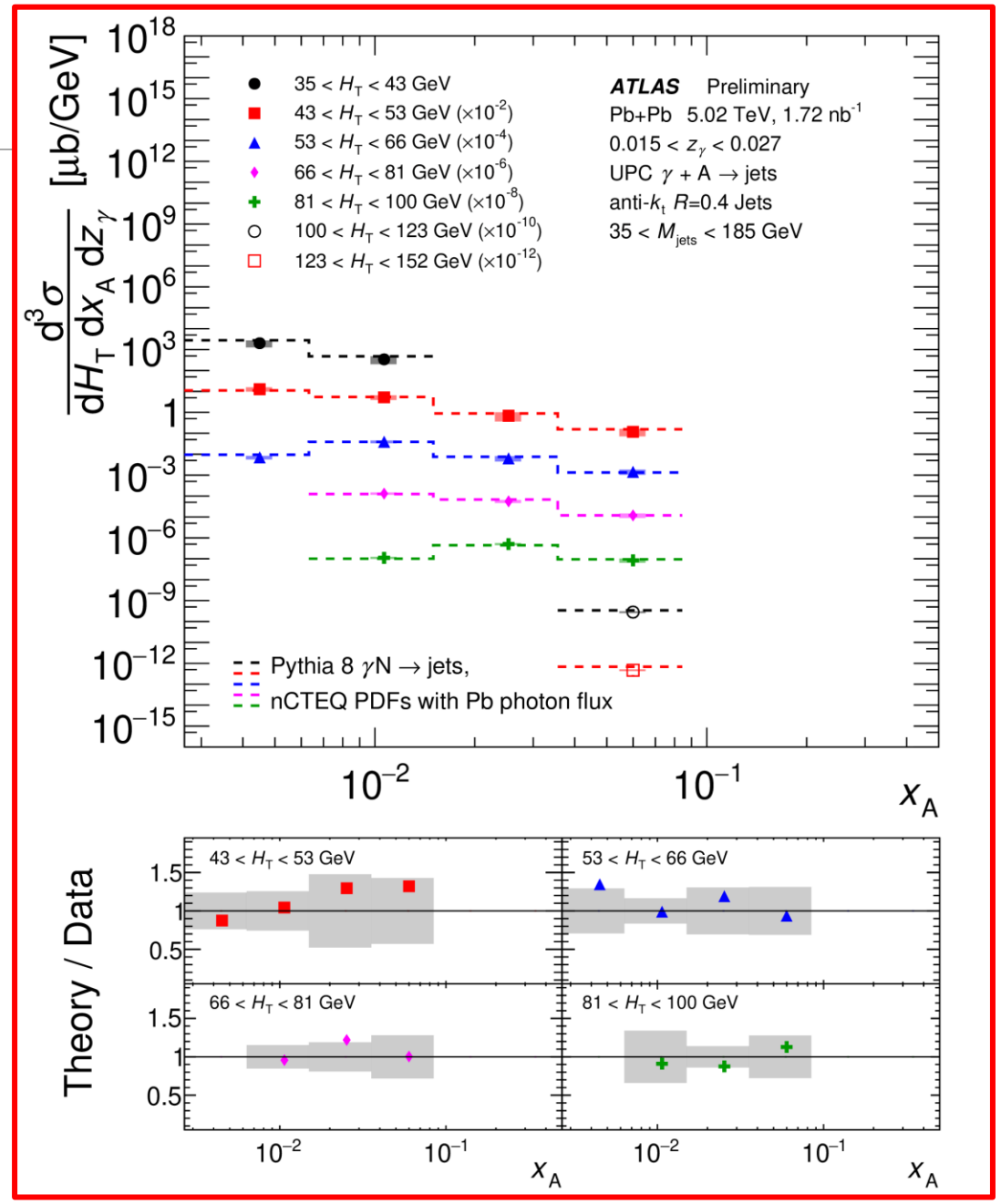

Systematic Uncertainties on Jet Cross-Sections

Systematics uncertainties are the key limiting factor in our sensitivity to nuclear PDFs.

The jet energy scale and resolution uncertainties are typically 5-10%.

Control over the preliminary low-μ calibration currently provides the dominant source of uncertainty.

Systematics uncertainties are also evaluated on the unfolding and event selections.

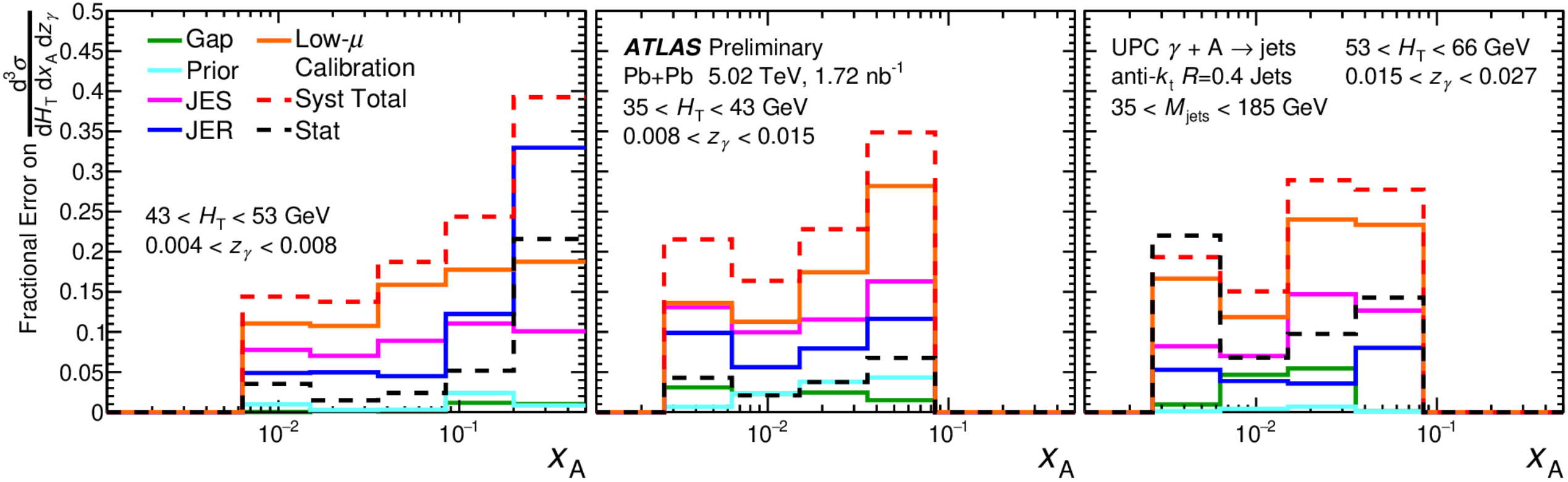

The Future of Photo-nuclear Measurements

- Photo-nuclear jet production is complimentary to inclusive DIS measurements at the EIC, which will probe lower x and Q^2.
  - UPC jet measurements will provide increasingly precise tests of saturation physics before the EIC turns on.
- Photo-nuclear flow at the EIC can be predicted using UPC results by varying the Q^2, as shown on the right.
  - UPC flow measurements at the LHC will provide a key baseline for precision EIC measurements to come.

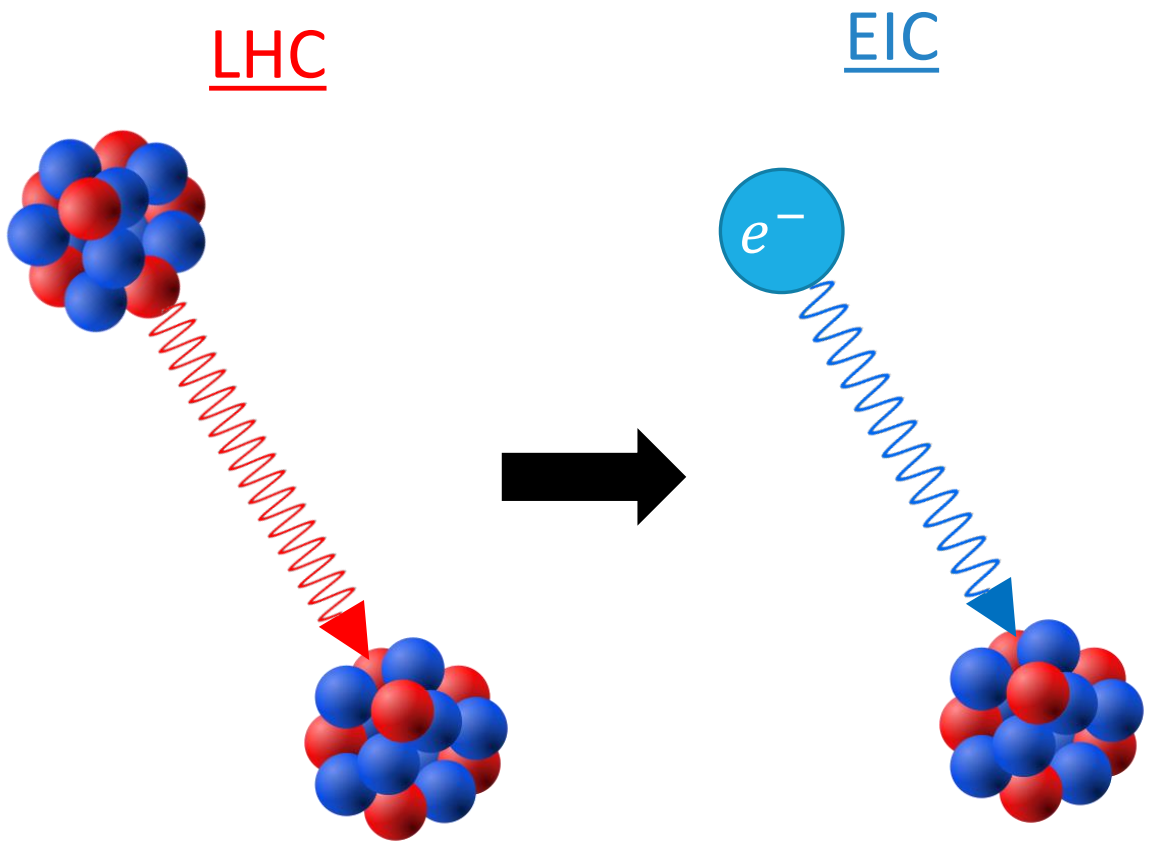

Shi et al., PRD 103, 054017 (2021)

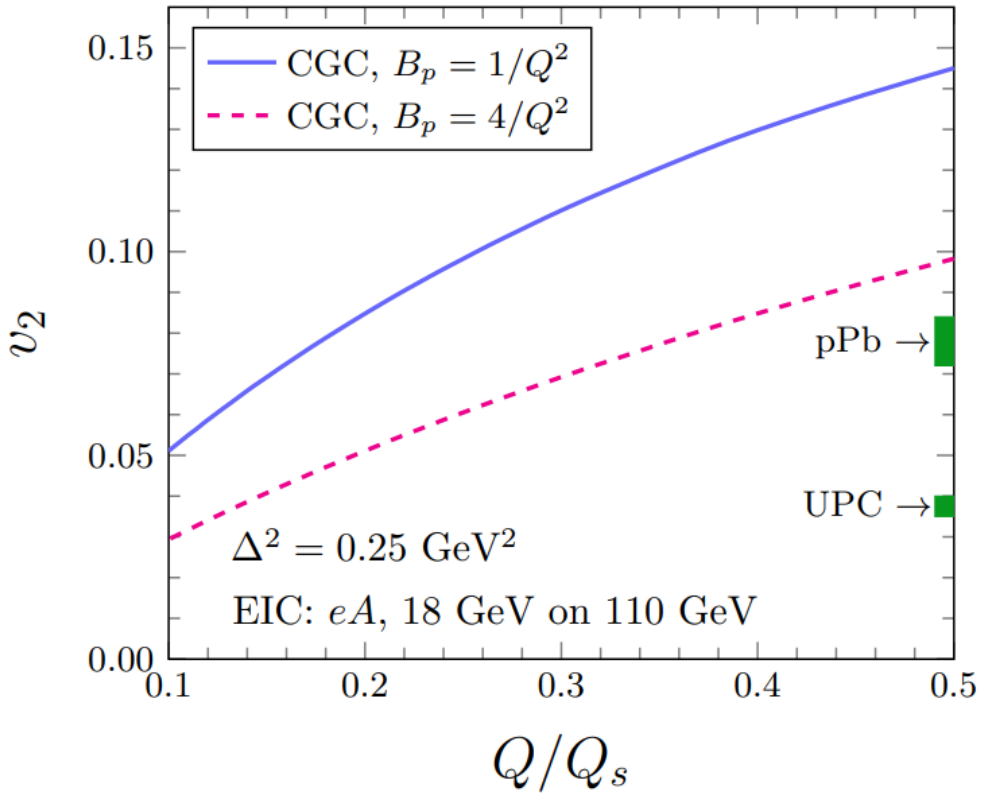

Conclusions

- Photo-nuclear dijet production was measured by ATLAS in 5.02 TeV Pb+Pb collisions with 2018 data.
  - This measurement has been fully unfolded for detector response for the first time.
  - Once final studies of low-μ jet response in ATLAS can be completed, substantial gains in systematic control can be achieved.
- Studies of 2-particle correlations in photo-nuclear collisions demonstrate collectivity in a novel small system.
  - These results can be effectively modelled as a rho-nucleus collision.
- Both measurements are connected to early physics goals for the EIC.

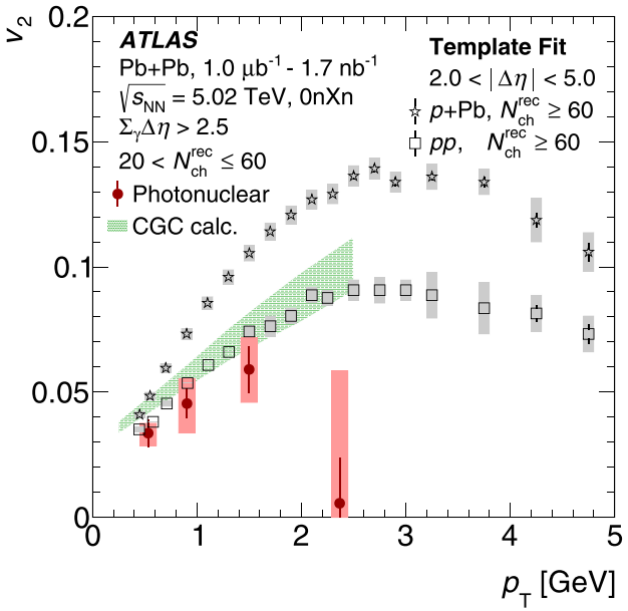

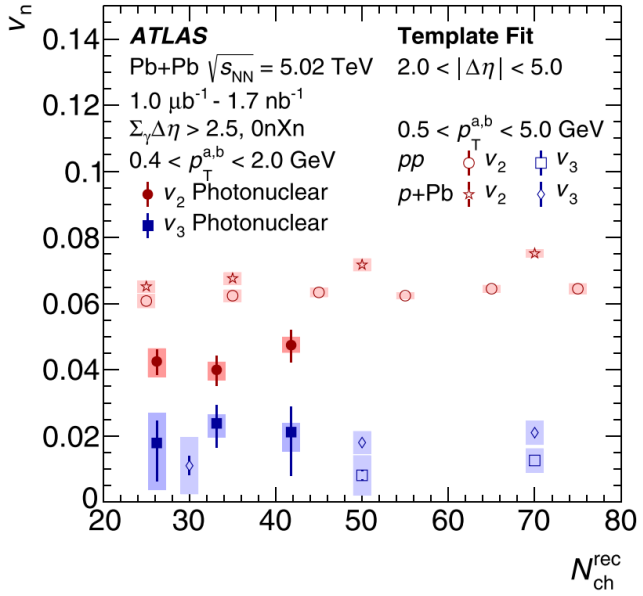

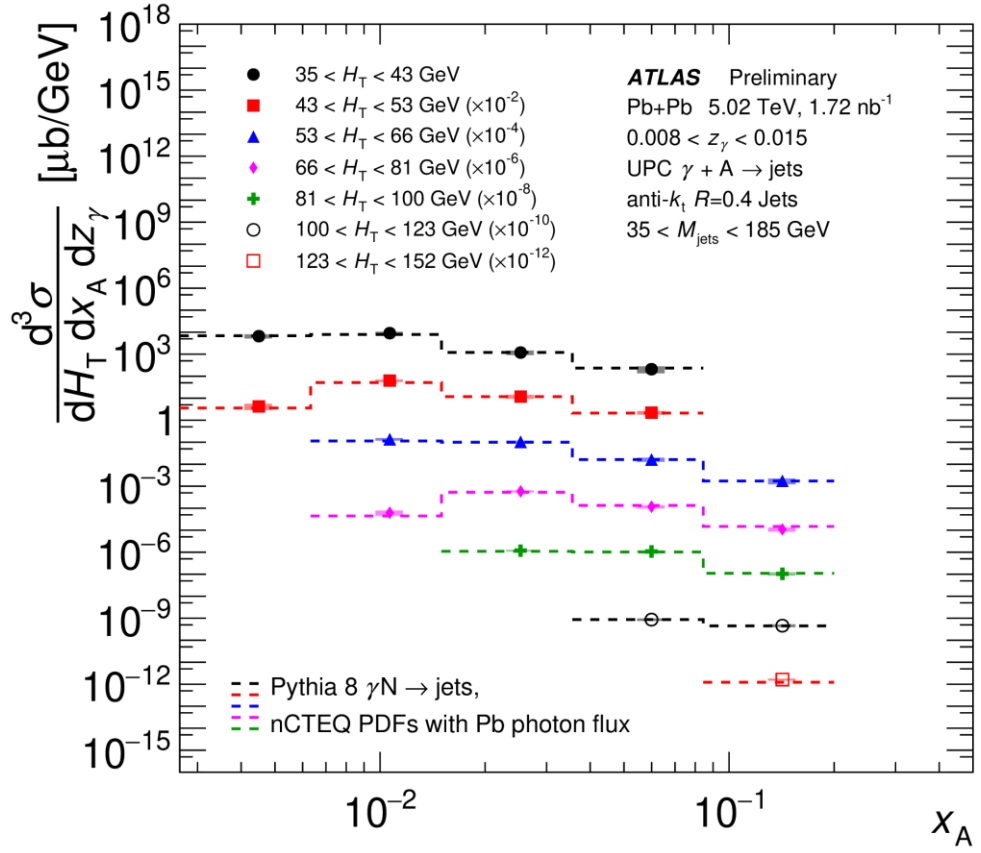

Backup

Importance of Neutron Topology: *0n0n* Events

For the first time, ATLAS has observed dijet production in UPC without nuclear breakup (0n0n).

Gaps are required on both sides of the detector: $\sum \Delta\eta > 2.0$

A factor of 10 more events are observed in data than are predicted from $\gamma\gamma \rightarrow$ jets, estimated by Pythia or comparison to $\gamma\gamma \rightarrow \mu^+\mu^-$ studies.

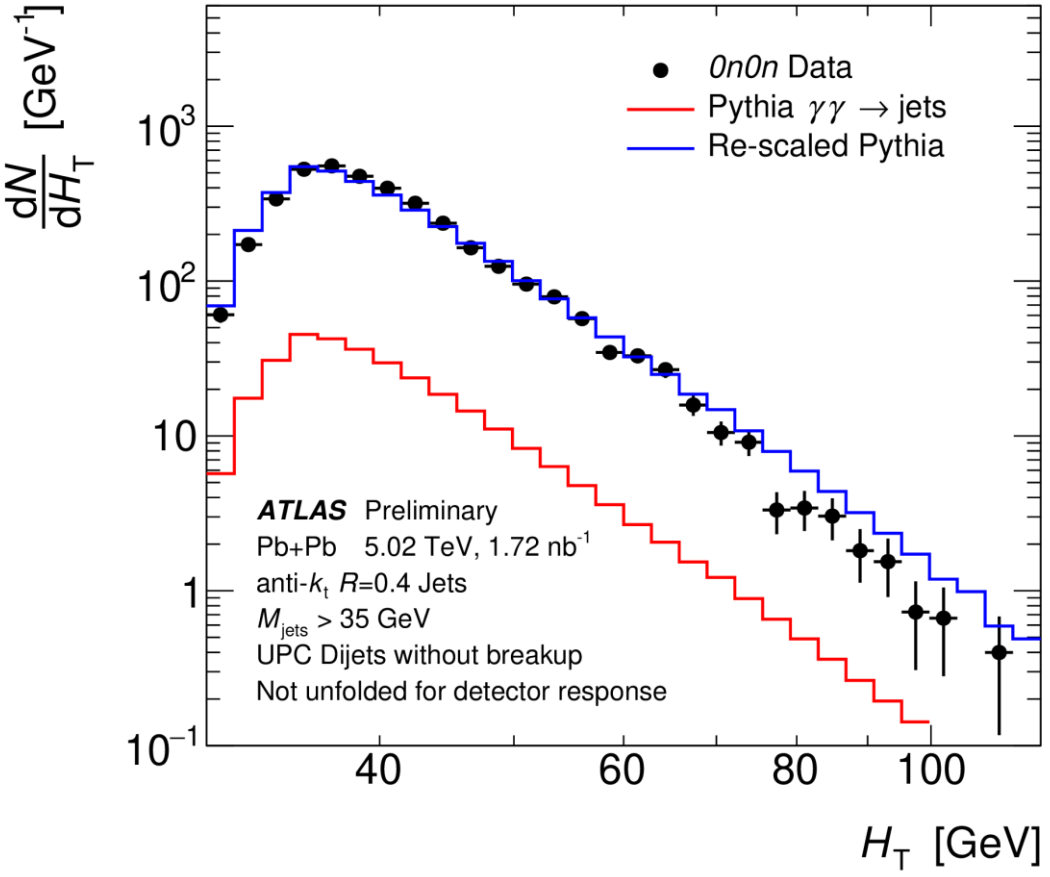

Importance of Neutron Topology: *0n0n* Events

For the first time, ATLAS has observed dijet production in UPC without nuclear breakup (0n0n).

Gaps are required on both sides of the detector: $\sum \Delta\eta > 2.0$

A factor of 10 more events are observed in data than are predicted from $\gamma\gamma \rightarrow$ jets, estimated by Pythia or comparison to $\gamma\gamma \rightarrow \mu^+\mu^-$ studies.

The distribution shapes look distinct from pure $\gamma\gamma \rightarrow$ jets.

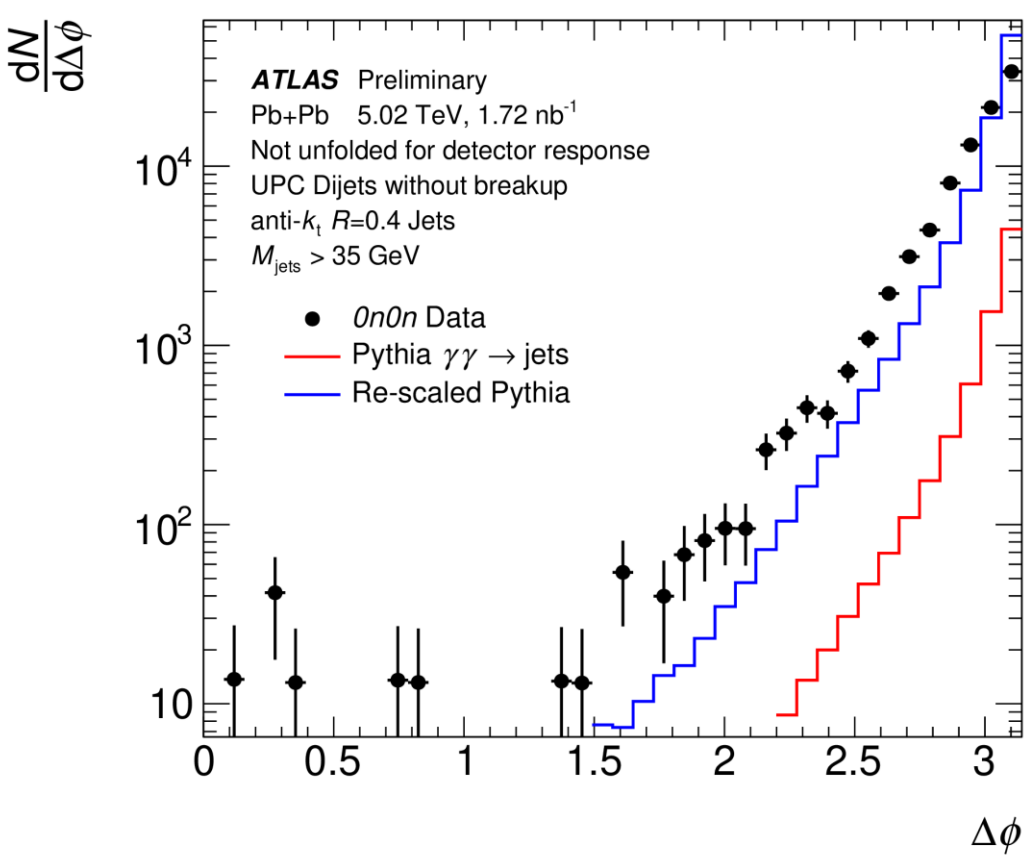

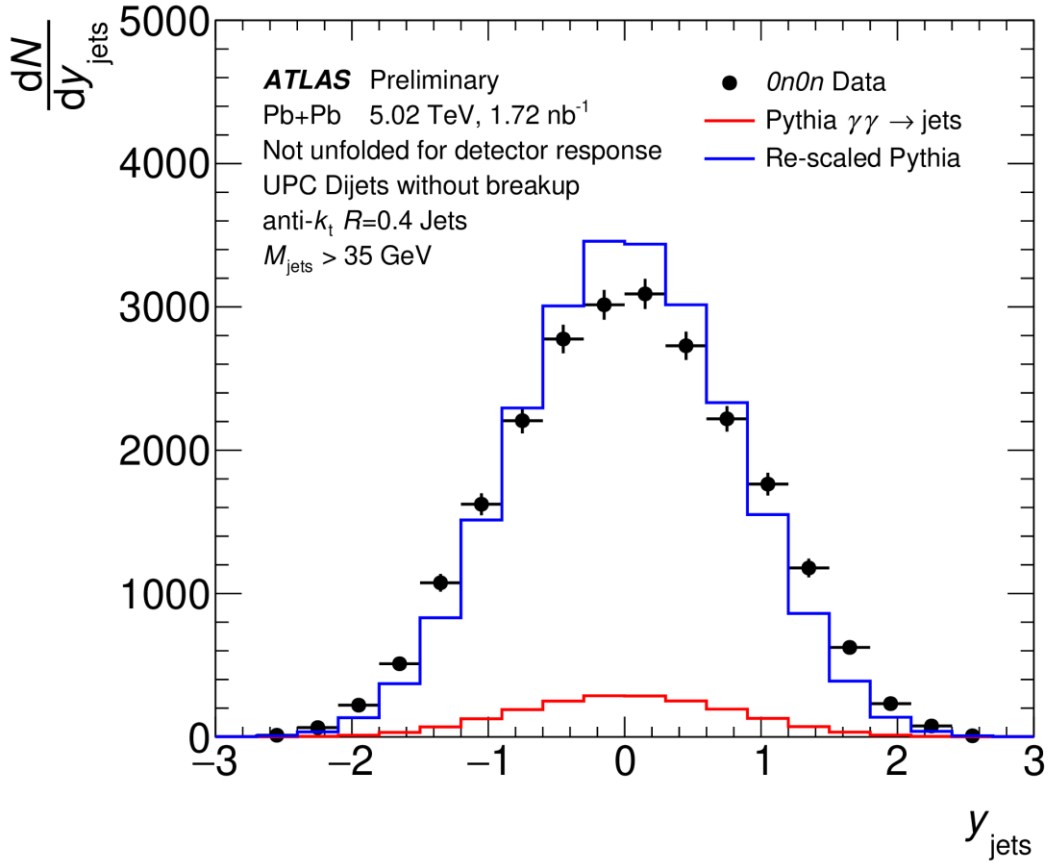

Constructing the Jet Cross-Section

$$\frac{d^3\sigma}{dH_T dx_A dz_\gamma} = \frac{1}{\mathcal{L}} \frac{\Delta Y}{\Delta H_T \Delta x_A \Delta z_\gamma}$$

H_T does not depend strongly on x_A and z_γ.

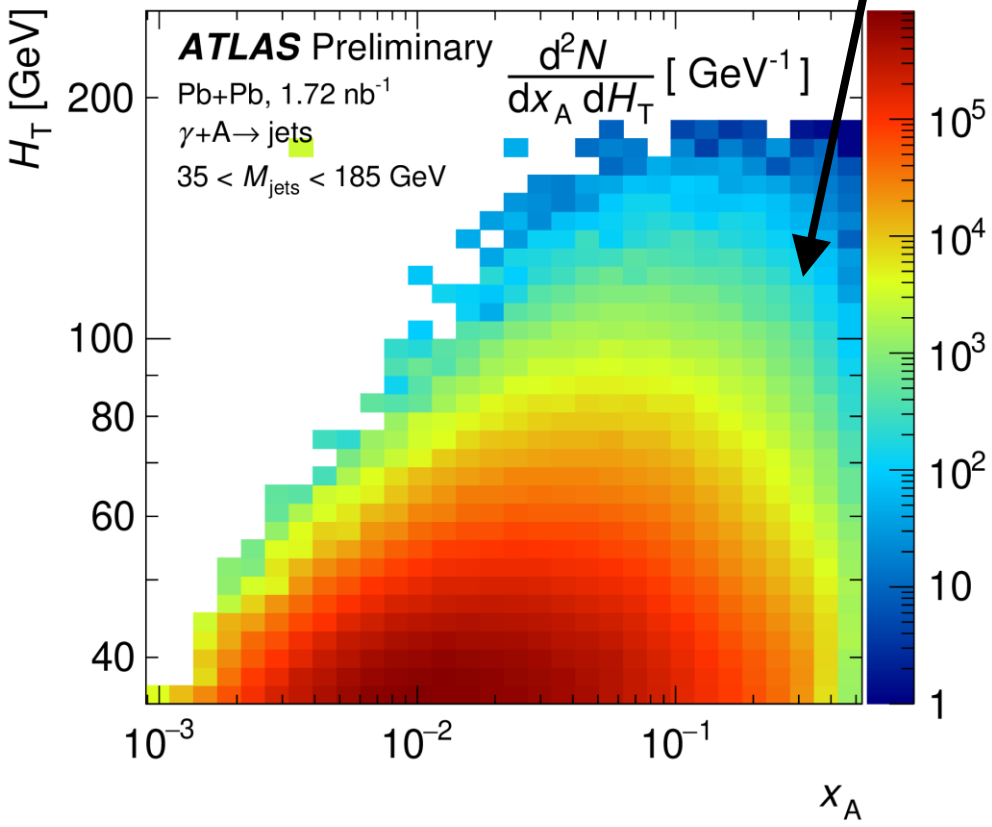

$$H_T \equiv \sum_i p_T^i$$

$$x_A \equiv \frac{M_{jets} e^{-y_{jets}}}{\sqrt{s_{NN}}}$$

$$z_\gamma \equiv \frac{M_{jets} e^{+y_{jets}}}{\sqrt{s_{NN}}}$$

x_A is strongly correlated with z_γ, yielding important acceptance effects in the two variables.

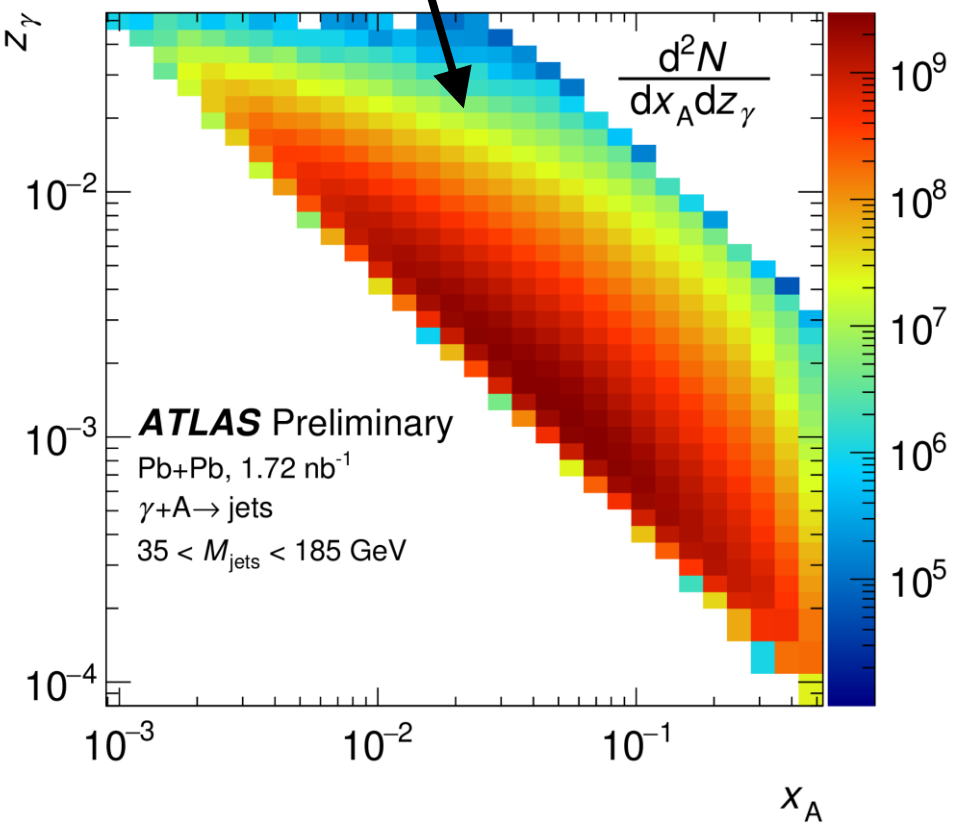

Unfolding Measured Jet Cross-Sections

The measured cross-sections are then unfolded in 3 dimensions to correct for detector effects.

- Low-p_T flavor effects are the largest correction.

$$H_T \equiv \sum_i p_T^i \quad x_A \equiv \frac{M_{jets} e^{-y_{jets}}}{\sqrt{s_{NN}}} \quad z_\gamma \equiv \frac{M_{jets} e^{+y_{jets}}}{\sqrt{s_{NN}}}$$

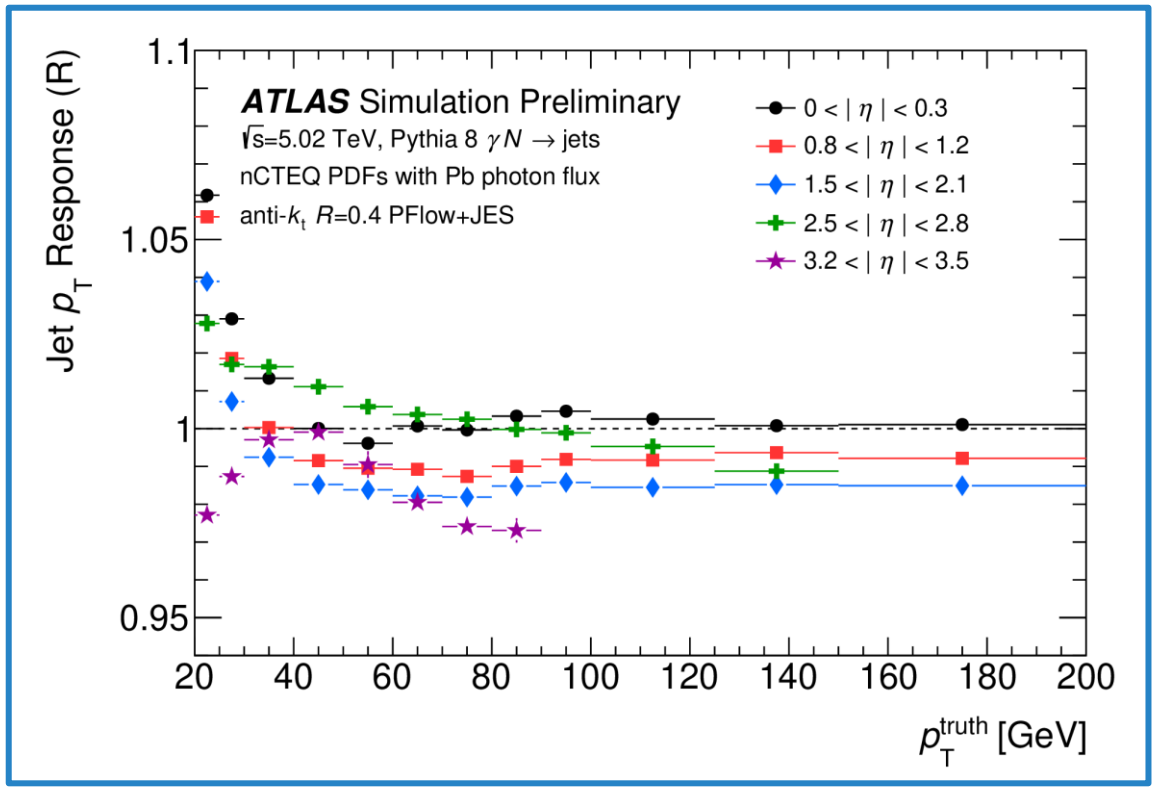

Unfolded / Measured

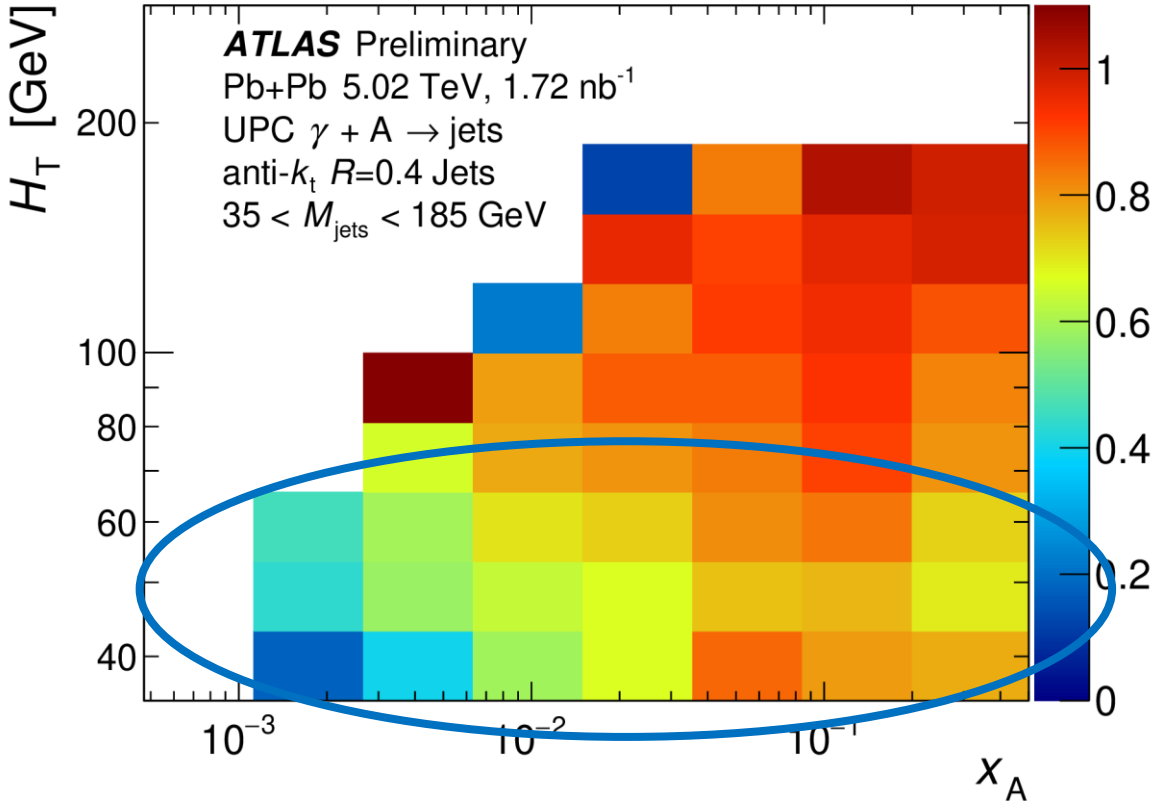

Measured Jet Cross-Sections

- At intermediate photon energies, we can access higher-x partons.

$$H_T \equiv \sum_i p_T^i \qquad x_A \equiv \frac{M_{jets} e^{-y_{jets}}}{\sqrt{s_{NN}}} \qquad z_\gamma \equiv \frac{M_{jets} e^{+y_{jets}}}{\sqrt{s_{NN}}}$$

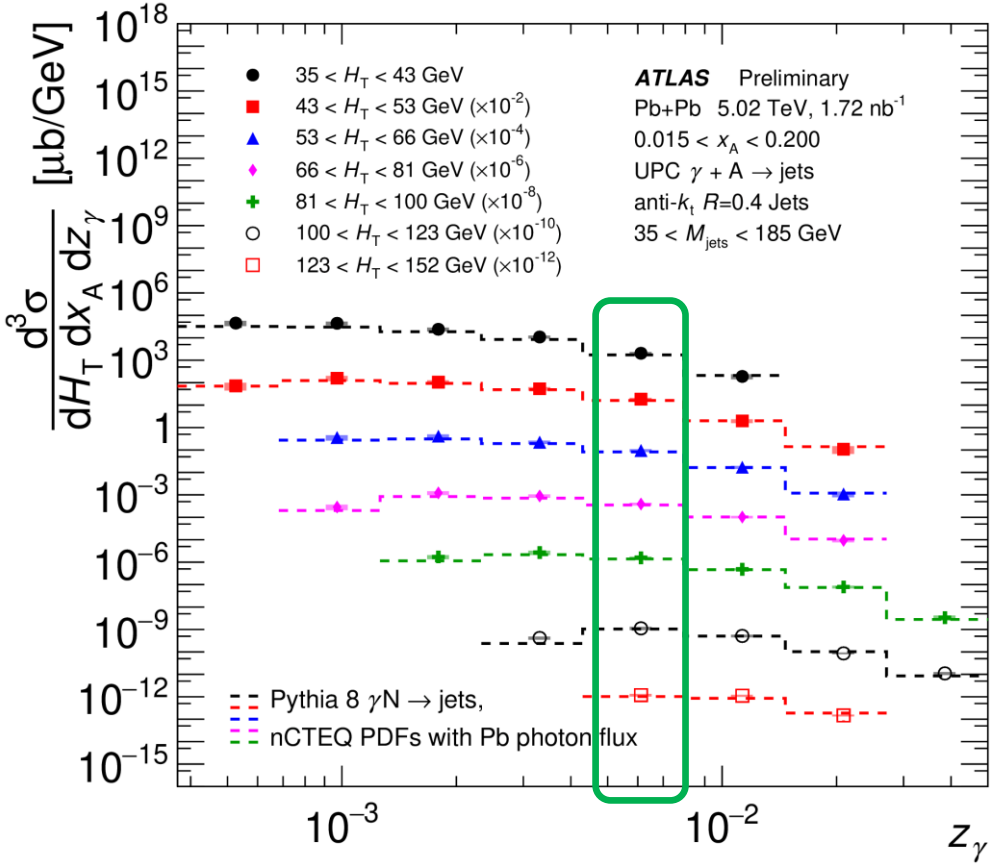

Photon Energy

$0.004 < z_\gamma < 0.008$

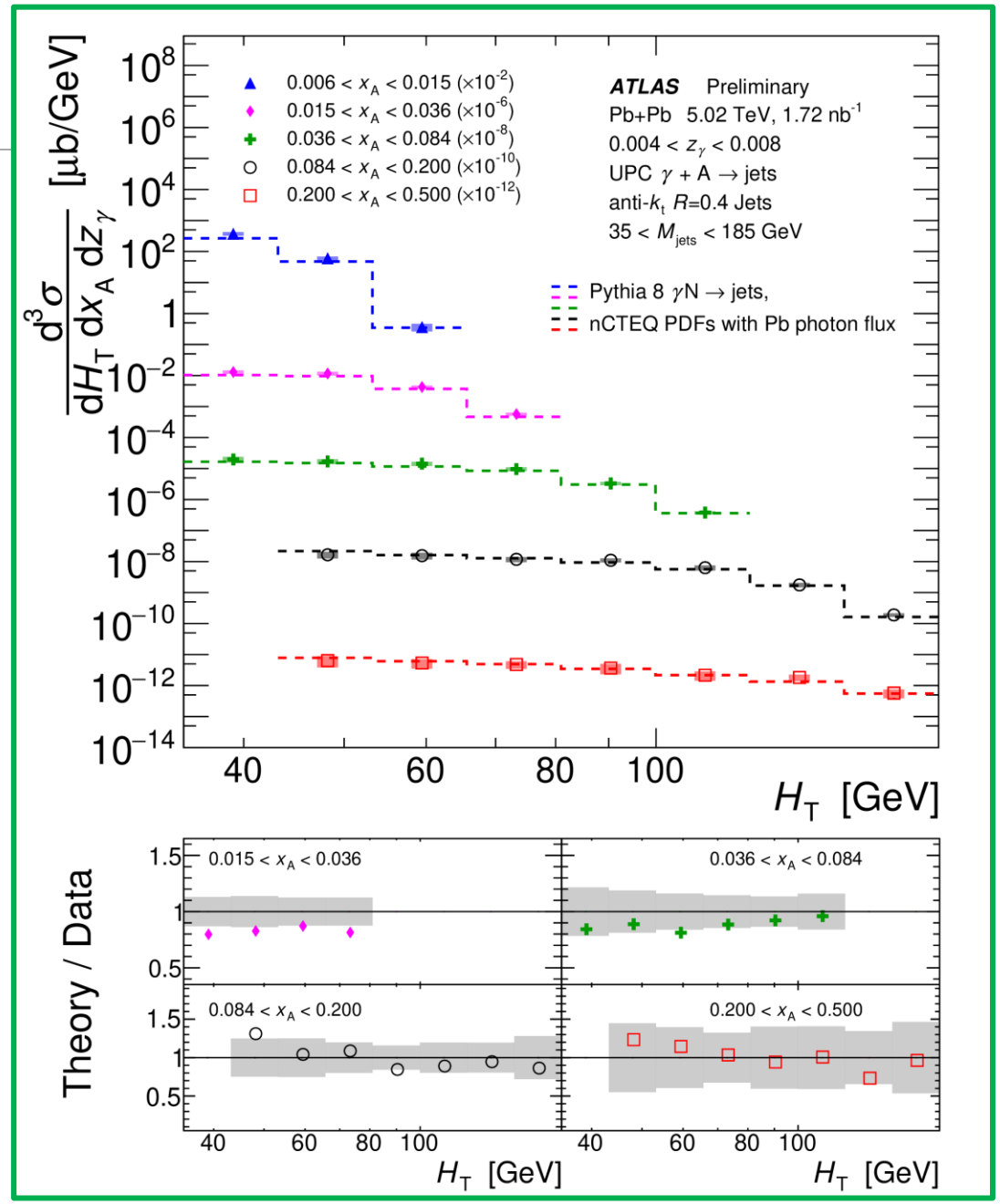

Measured Cross-Sections

- Going higher in photon energy opens up the low-x shadowing region.
- Results are quite consistent with the theoretical model.

$$H_T \equiv \sum_i p_T^i \qquad x_A \equiv \frac{M_{jets} e^{-y_{jets}}}{\sqrt{s_{NN}}} \qquad z_\gamma \equiv \frac{M_{jets} e^{+y_{jets}}}{\sqrt{s_{NN}}}$$

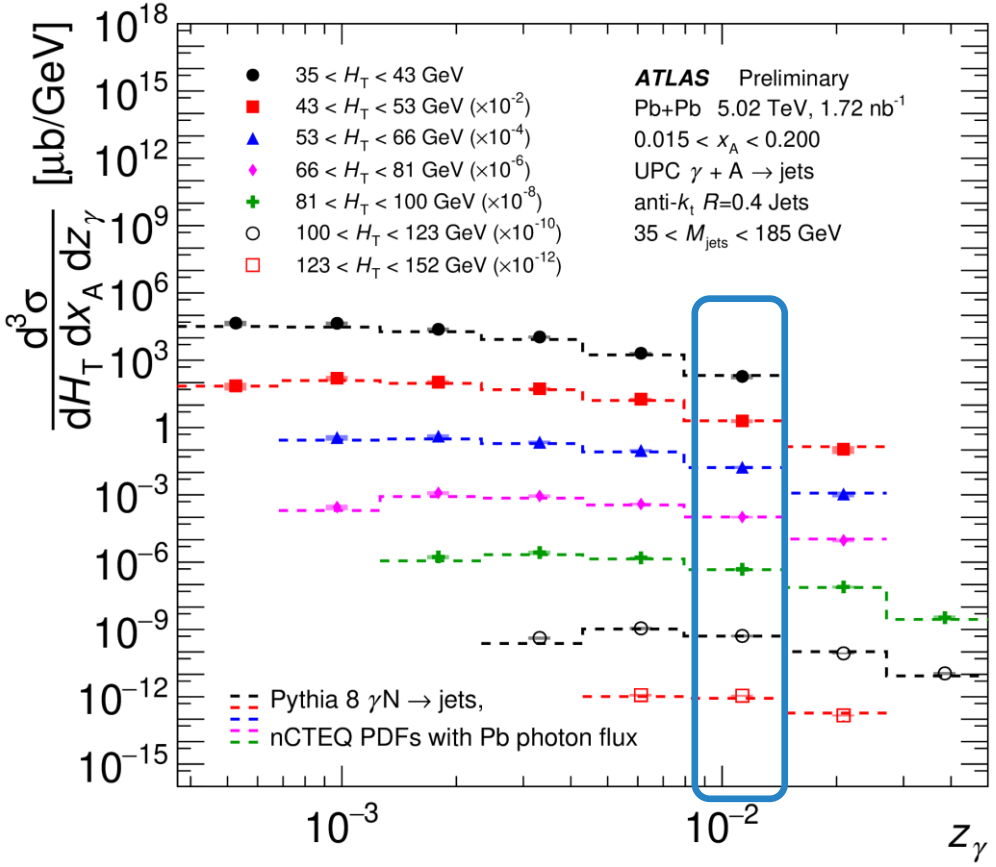

Photon Energy

$0.008 < z_\gamma < 0.015$

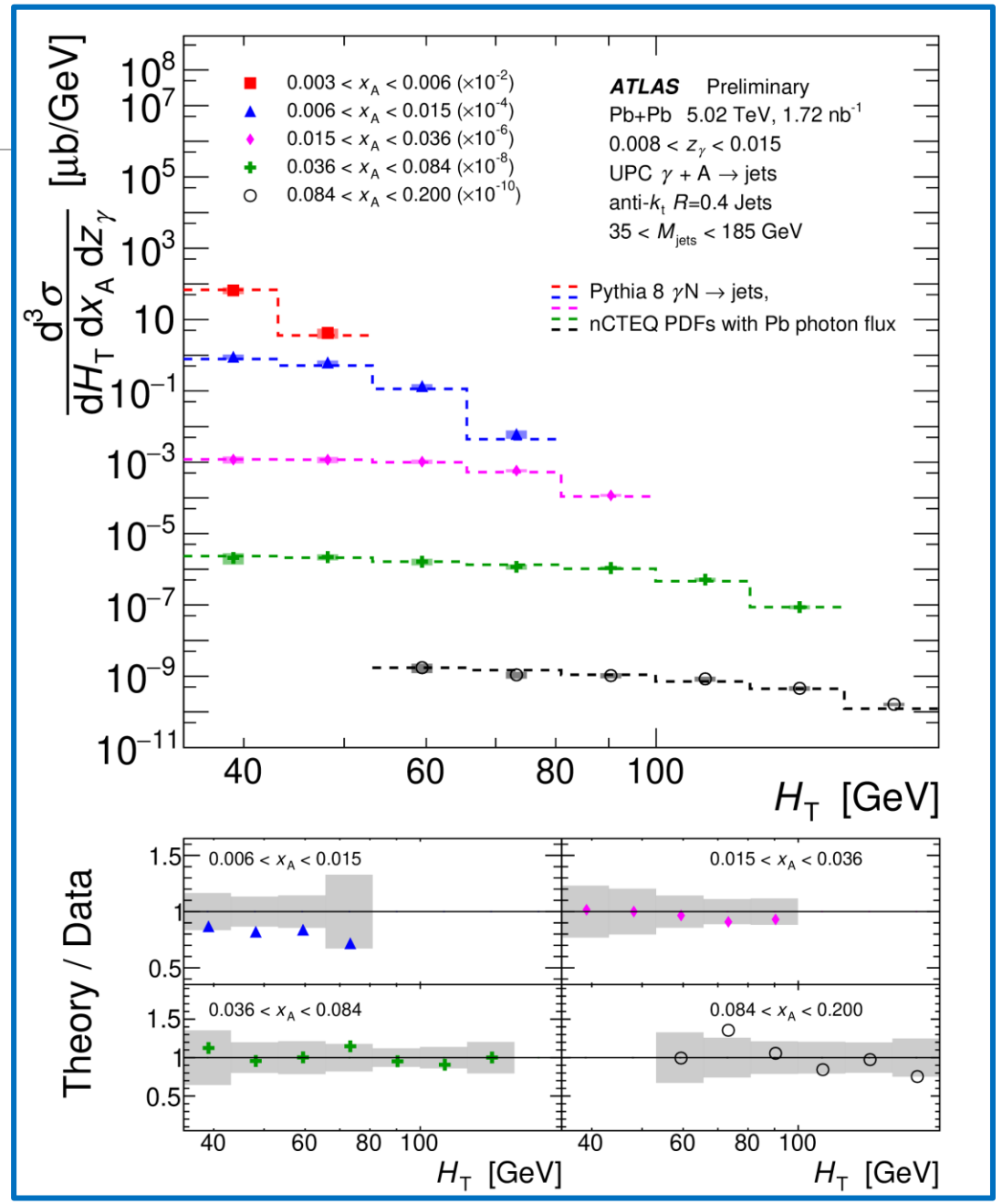

Measured Cross-Sections

- The highest photon energy allows the most access to low-x.
- Systematic control is more of a challenge near acceptance edges.

$$H_T \equiv \sum_i p_T^i \qquad x_A \equiv \frac{M_{jets} e^{-y_{jets}}}{\sqrt{s_{NN}}} \qquad z_\gamma \equiv \frac{M_{jets} e^{+y_{jets}}}{\sqrt{s_{NN}}}$$

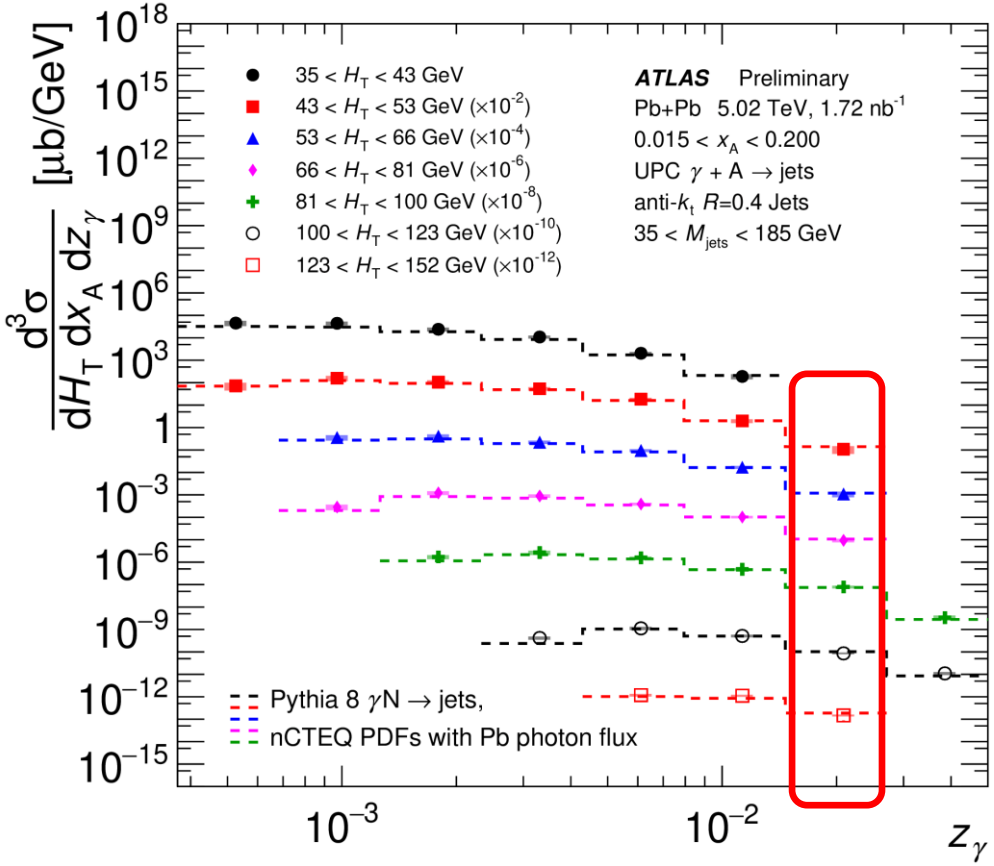

Photon Energy

$0.015 < z_\gamma < 0.027$